AN ALTERNATIVE DIFFERENTIAL PROTECTION SCHEME FOR ELECTRICAL MICROGRIDS

GISELA SOUSA FERREIRA

MASTER THESIS ON ELECTRICAL ENGINEERING

TECHNOLOGY FACULTY

UNIVERSITY OF BRASÍLIA

Universidade de Brasília

Faculdade de Tecnologia

Departamento de Engenharia Elétrica

An Alternative Differential Protection Scheme for Electrical Microgrids

Gisela Sousa Ferreira

Dissertação de mestrado submetida ao Departamento de Engenharia Elétrica da Faculdade de Tecnologia da Universidade de Brasília, como parte dos requisitos necessários para a obtenção do grau de mestre.

APROVADO POR:

Prof. Francis Arody Moreno Vásquez, D.Sc. (ENE-UnB)
(Orientador)

Prof. Kleber Melo e Silva, D.Sc. (ENE-UnB)
(Examinador Interno)

Prof. José Carlos de Melo Vieira Júnior, D.Sc. (EESC-USP)
(Examinador Externo)

Brasília/DF, 13 de maio de 2024.

FICHA CATALOGRÁFICA

GISELA SOUSA FERREIRA

An Alternative Differential Protection Scheme for Electrical Microgrids. [Distrito Federal] 2024.

xiii, XXp., 210 x 297 mm (ENE/FT/UnB, mestre em Engenharia Elétrica, 2024).

Dissertação de Mestrado – Universidade de Brasília, Faculdade de Tecnologia.

1. Proteção Diferencial
2. Microrredes Elétricas
3. Sistema Elétrico de Potência
4. EMTP-RV

I. ENE/FT/UnB

II. Título (série)

REFERÊNCIA BIBLIOGRÁFICA

FERREIRA, G. S. (2023). An Alternative Differential Protection Scheme for Electrical Microgrids, Dissertação de Mestrado em Engenharia Elétrica, Publicação PPGEE.DM - 810/24, Departamento de Engenharia Elétrica, Universidade de Brasília, Brasília, DF, 120p.

CESSÃO DE DIREITOS

AUTOR: Gisela Sousa Ferreira

TÍTULO: An Alternative Differential Protection Scheme for Electrical Microgrids

GRAU: Mestre ANO: 2024

Gisela Sousa Ferreira

Departamento de Eng. Elétrica (ENE) - FT

Universidade de Brasília (UnB)

Campus Darcy Ribeiro

CEP 70919-970 - Brasília - DF - Brasil

"To strive,

to seek,

to find,

and not to yield"

by ALFRED, LORD TENNYSON

ACKNOWLEDGEMENTS

Firstly, I would like to thank God for been everything to me. To support, love and solace me.

To my family, who is my rock in this world and the love that I feel for her is immeasurable.

I am extremely thankful to my advisor, Dr. Francis Arody, for giving me the opportunity to work on this master thesis and to believe in me, during all the guidance. He is a great professional and it was an honor to work with him. Without him I couldn't have done this master thesis.

Finally, I am thankfully for one person who encourage me to be always a better version of me.

ABSTRACT

This work presents a new protection function for microgrids based on differential current, with a smaller number of current transformers (CT) than in the conventional approach, complemented by a dead zone logic and an adaptive minimum operating current element. To achieve this objective, a medium voltage (MT) microgrid was modeled and simulated using the EMTP program. The algorithm was computationally implemented and simulations were carried out to test its effectiveness, supported by the correct definition of protection zones as a relevant aspect. The results demonstrated that the proposed method responds reliably and safely to various types of short-circuits that occur in different locations of the microgrid, with several fault impedances, at the same time. Furthermore, its robust performance has been confirmed under different operating conditions, including on-grid and off-grid modes, as well as ring and radial topologies. The proposed protection method represents a viable alternative for the protection of microgrids due to its simplicity, independence from the generation-load balance, the need of fewer current transformers compared to traditional differential protection scheme, and its dependability and security. Furthermore, although the number of CTs is smaller than there would be conventionally for a differential element, the backup logic for dead zones ensures that the microgrid is logically, and physically, covered by the complete protection scheme.

Keywords: Converter-based sources; Dead Zone; Differential Protection; Electrical Microgrids; Incremental Quantities; Renewable Sources.

RESUMO

UM ESQUEMA DE PROTEÇÃO DIFERENCIAL ALTERNATIVO PARA MICROREDES ELÉTRICAS

Este trabalho apresenta uma nova função de proteção para microrredes baseada na corrente diferencial, com um número de transformadores de corrente (TC) menor do que na abordagem convencional, complementada por uma lógica de zona morta e um elemento adaptativo de corrente mínima de operação. Para atingir este objetivo, uma microrrede de média tensão (MT) foi modelada e simulada utilizando o programa EMTP. O algoritmo foi computacionalmente implementado e foram efetuadas simulações para testar a sua eficácia, sempre colocando como aspecto relevante a definição das zonas de proteção. Os resultados demonstraram que o método proposto responde de forma confiável e segura a vários tipos de curtos que ocorrem em diferentes locais da microrrede, com diferentes valores de impedância de falta, em tempo simultâneo. Além disso, o seu desempenho robusto foi confirmado em diferentes condições operacionais, incluindo os modos on-grid e off-grid, bem como topologias em anel e radiais. O método de proteção proposto representa uma alternativa viável para a proteção de microrredes devido à sua simplicidade, independência do balanço geração-carga, à menor necessidade de transformadores de corrente em comparação com os esquemas de proteção diferencial tradicionais e à sua confiabilidade e segurança globais. Ainda, embora o número de TCs seja menor do que haveria convencionalmente para um elemento diferencial, a lógica de retaguarda para zonas mortas garante que a microrrede seja logicamente, e fisicamente, coberta pelo esquema completo de proteção.

Palavras-chave: Fontes baseadas em conversor; Zona morta; Proteção Diferencial; Microrredes Elétricas; Quantidades Incrementais; Fontes renováveis.

CONTENTS

Table of Contents i

List of figures iii

List of tables v

List of symbols vi

Glossary vii

Chapter 1 – Introduction 1

1.1 Background 1
1.2 Motivation 3
1.3 Objectives 3
1.4 Publications 4
1.5 Thesis Organization 4

Chapter 2 – Literature Review 5

Chapter 3 – Theoretical Background 14

3.1 Conventional Differential Protection 14
3.2 Control Of Three-phase Inverters 16
3.2.1 PQ MODE 17
3.2.2 V/F MODE 19

Chapter 4 – Proposed Protection Function 20

4.1 Proposed Protection System 20
4.1.1 Main Protection Logic Description 22
4.1.2 Adaptive Minimum Threshold Logic 23
4.1.3 Backup Dead Zone Protection Logic 25

4.2 Signal Processing 27

Chapter 5 – Results and Discussion 29

5.1 Electrical Microgrid Model Description 29
5.2 Protection Zones 31
5.3 Case 1: Phase-to-phase fault (On-grid and off-grid operation) 32
5.4 Case 2: Short-circuit at dead zone 38
5.5 Case 3: Influence of fault resistance 39
5.6 Case 4: Fault types 41
5.7 Case 5: Ring and radial topology 43
5.8 Case 6: Simultaneous short-circuits 44
5.9 Contributions 48

Chapter 6 – Conclusions and Future Works 50

References 52

LIST OF FIGURES

3.1 Traditional Differential Current Protection Scheme. 15

3.2 On-grid PQ mode 18

3.3 Off-grid V/f mode. 19

4.1 Proposed Scheme 21

4.2 Main protection logic of the proposed algorithm. 23

4.3 Response of the adaptive minimum pickup strategy. 25

4.4 Backup logic of the proposed algorithm for dead zone protection 27

5.1 Proposed Grid System 30

5.2 Test microgrid modeled in the software EMTP. 32

5.3 Short-circuit AB in Z1 off-grid operation: $I_{op} \times I_{res}$ 33

5.4 Short-circuit AB in Z1 off-grid operation: $\Delta I_{op} \times t$ 34

5.5 $I_{res}.SLP \times I_{op}-$Fault AB in Z1$-Off-grid.$ 34

5.6 Case 01. Time domain response of the proposed function 87. Off-grid operation. 35

5.7 Case 01. Time domain response of the traditional function 87. Off-grid operation. 35

5.8 Short-circuit AB in Z1 on-grid operation: $I_{op} \times I_{res}$ 36

5.9 Short-circuit AB in Z1 in on-grid operation: $\Delta I_{op} \times t$ 36

5.10 $I_{res}.SLP \times I_{op}-$Fault AB in Z1$-On-grid.$ 37

5.11 Case 01. Time domain response of the proposed function 87. On-grid operation. 37

5.12 Case 01. Time domain response of the traditional function 87. On-grid operation. 38

5.13 Case 2a: Fault if the dead zone close to CT2. 39

5.14 Case 2b: Fault if the dead zone close to CT6. 39

5.15 Case 3 - Fault resistance impact. (a) $I_res.SLP \times I_op$ $(b) Operation flags$. 40

5.16 Case 3 - Fault resistance impact. (a) $I_res.SLP \times I_op$ $(b) Operation flags$. 41

5.17 Case 04. Relay operation in zones Z3 and Z4 in case of a fault AG in Z4. 41

5.18 Case 04. Relay operation in zones Z3 and Z4 in case of an fault ABG in Z4. 42

5.19 Case 04. Relay operation in zones Z3 and Z4 in case of fault ABC in Z4. 42

5.20 Case 04. Relay operation in zones Z3 and Z4 in case of a fault AG in Z4. 43

5.21 Case 04. Time-domain response of ΔI_op of Z3 and Z4 in case of a fault ABC in Z4. 43

5.22 Case 05. Relay response for a CG fault in Z5 with a microgrid ring topology. 44

5.23 Case 05. Relay response for a CG fault in Z5 with a radial microgrid. . 44

5.24 Case 06. Response in the traditional operational plane. 45

5.25 Case 06. Operation flags in phase B for the traditional 87 element. . . . 45

5.26 Case 06. Operation flags in phase C for the traditional 87 element. . . 46

5.27 Case 06. Response in the operational plane of the proposed scheme. . . 46

5.28 Case 06. Operation flags in phase B for the proposed 87 element. . . . 47

5.29 Case 06. Operation flags in phase C for the proposed 87 element. . . . 47

LIST OF TABLES

2.1 Summary of Research Works - Mode Operation and Topology. 11

2.2 Summary of Research Works - Number of CTs. 12

2.3 Summary of Research Works - Fault Resistance, Tripping and Loads. . 13

5.1 Parameters of the Simulated Power System Components 30

5.2 Parameters of the Simulated Power System Components - Loads 31

5.3 Protection zones (CTs, CBs) and common CTs. 32

LIST OF SYMBOLS

$C_{dc-link}$	DC-Link capacitors
$f_{droop,ref}$	Droop Reference Frequency
I_{op}	Operation Current
I_{res}	Restriction Current
$I_{op,min}$	Minimum Operation Current
i_g	Grid Currents
$V_{droop,ref}$	Droop Reference Voltage
V_g	Grid Voltage
dq/abc	Clarke's transform
abc/dq	Park's transform

GLOSSARY

AC	Alternating Current
ANSI	American National Standards Institute
CB	Circuit Breaker
CBDG	Distributed Generation Circuit Breaker
CT	*Current Transformer*
CTDG	*Distributed Generation Current Transformer*
DC	Direct Current
DG	Distributed Generation
DL	Line Distribution
EMTP	Electromagnetic Transient Program
FDD	Fault Detection and Diagnostics
IEEE	Instituto de Engenheiros Eletricistas e Eletrônicos
L	Load
MG	Microgrid
MPPT	Maximum Power Point Tracking
MV	Medium Voltage
ONS	National Electric System Operator
PI	Proportional-Integral controller
PLL	Phase Locked Loop

P/Q	Reactive Power Control
SIN	National Interconnected System
SLP	Slope
V/F	Speed/Frequency control
Z	Protection Zone

CHAPTER 1

INTRODUCTION

1.1 BACKGROUND

The growing insertion of intermittent renewable sources represents a sustainable alternative for electric energy generation as centralized or distributed generation (DG). Nevertheless, it brings operation challenges because of their uncontrollable nature and variability. As the transition of the electrical energy matrix progresses for the triennium 2025/27, the National System Operator (ONS..., 2020) anticipates the introduction of new energy sources and technologies. This shift will bring innovative approaches to utilizing generation sources, challenging existing paradigms. In 2022, the estimated distributed generation of the National Interconnected System (SIN) was 16 GW. Drawing attention to the Northeast in Brazil, it is noteworthy that on 21/10/22, at 10 am, there was a record-breaking solar photovoltaic generation, reaching an average hourly output of 3,667 MW. This achievement accounted for 31% of the load being supplied by this source. Furthermore, on 19/10/22, at 10 pm, there was a record for wind generation, reaching an average hourly output of 16,656 MW, representing 124.65% of the region's load supplied by this source (ONS..., 2022).

The increasing connection of distributed generation units to traditional distribution networks has led to changes in the usual way of protecting these grids. Specifically, the implantation of electrical microgrids, based on distributed loads and generation units, is an actual concern once the fault nature of inverter-based sources and the grid flexibility can compromise the traditional protection methods. For example, distribution networks are designed on the basis of large short circuits currents with a radial (unidirectional) power flow (WHEELER *et al.*, 2017). However in new dynamic configurations, other variables can contribute to the protection of these microgrids: the

topology, which can be ring or radial; the modes of operation, connected to the grid or islanded; the positioning of loads; the bi-directionality of the power flow; the intermittency of distributed generation and how these characteristics alter short circuits, even if they are not directly involved in the fault.

In this context, differential current-based protection, widely used for high-voltage equipments, is a widespread concept used to develop new protection algorithms in microgrid applications. This method uses the principle that under normal conditions, the current that enters a grid is the same that will leave the grid. Consequently, differential current, which is the difference between the currents entering and leaving the grid, shall be zero. Nevertheless, this will not occur when an internal fault happens, and a non-zero differential current is used on a fault condition detection (LOUW *et al.*, 2014). The differential protection function is commonly used in commercial relays for power system equipment and transmission lines. It is a challenge to improve and use the technique for protection of microgrids maintain flexibility, sensibility, selectivity, feasibility, coordination and velocity. Furthermore, conventional radial networks use one CT and one circuit breaker on each distribution line for coordinated overcurrent protection, besides other forms of protection, like fuses and reclosers. However, renewable sources could make this type of configuration inappropriate due to variable short-circuit levels.

In that sense, this thesis presents a suitable approach to implement the traditional differential current element using less quantity of CTs, reinforced by an incremental current-based strategy to avoid malfunctions in distribution lines. In addition, dead zones must be also covered so an additional strategy must be considered. On the other hand, the algorithm must provide dependability and security for on-grid and off-grid operations with radial and ring configurations aiming to represent a suitable alternative for microgrid protection.

1.2 MOTIVATION

With the growth of renewable sources plants in conventional distribution networks, it is necessary to develop new protection techniques, as several variables become part of the network. The type and quantity of generation units, the mode of operation, the bidirectional power flow, and the network topology are some of them.

The list of factors can jeopardize the correct performance of relaying algorithms is large, and several proposals try to consider all of them. In that sense, new algorithms could be unfeasible for commercial relay applications due to the quantity of information. For this reason, a traditional concept, but considering the particularities of the grid to be protected, can still be used to develop protection algorithms without requiring more advanced technology. Nevertheless, it must be recognized that communication systems have a relevant role for the correct implementation of a microgrid protection scheme due to the presence of instrument transformers in different locations.

It is worth mentioning that improving the protection of electrical microgrids is still a challenge for power systems worldwide. In this context, the main motivation of this dissertation is to contribute to the safety and reliability of the energy delivered to the consumer. In that sense, the protection studies by using the differential current concept is an opportunity for understanding and implementing algorithms in the network which is more efficient with tangible cost.

1.3 OBJECTIVES

This work aims to develop an alternative protection algorithm for microgrid applications, based on the differential current principle, for a medium voltage flexible microgrid with converter-interfaced sources and distributed loads. In order to carry out this study some specific objectives are set out:

- Model a microgrid in the EMTP software (Electromagnetic transients program), aiming to simulate on-grid and off-grid operation, as well as different flexible configurations.

- Implement the conventional differential current-based protection algorithm
- Introduce the proposed relaying technique and compare its performance with the traditional approach.
- Identify the advantages and limitations of the new protection algorithm.

1.4 PUBLICATIONS

The studies developed throughout the master's degree enabled the publication of the following article, which is directly related to the theme of the master's degree:

- Gisela Sousa Ferreira, Francis Arody Moreno Vásquez, A new current-based protection system for inverter-dominated microgrids, Electric Power Systems Research, Volume 225, 2023, https://doi.org/10.1016/j.epsr.2023.109814.

1.5 THESIS ORGANIZATION

The present work is organized as follows:

- Chapter 2 provides a brief presentation of the main protection articles proposed in the highly relevant literature, as well as a concise assessment of them in relation to their advantages and disadvantages;
- Chapter 3 provides a theoretical principles about the topics addresses in this thesis, serving as the basis for the document understanding;
- Chapter 4 describes and explains the proposed protection technique;
- Chapter 5 exposes case studies and results;
- Chapter 6 exposes the thesis conclusions and proposes future works.

CHAPTER 2

LITERATURE REVIEW

The emergence of electrical microgrids as a new concept of power distribution and generation systems inspires the development of new forms of protection. Aiming to overcome the inverter challenges mentioned in previous section, alternative relaying algorithms were developed for microgrids.

Despite the infrastructure and operation characteristics of microgrids, protection algorithms based on conventional power systems functions such as differential, directional, and overcurrent are still the basis for this proposed technique. Independently, the protection element used is influenced by topology and operating mode. These flexibility characteristics of microgrids, help to test the effectiveness of the algorithm.

This chapter presents some works that deal with differential protection of microgrids, in order to validate this study and identify some views on this topic. For this purpose, the techniques used are briefly described and the main results are mentioned. Furthermore, observations were made regarding obstacles encountered in the development of the proposed methods. Besides that, tables are presented with summaries of the work, the main characteristics of the proposed methods, in addition to aspects evaluated by them. Finally, the aspects cited in works were also used for comparison to show the validity of the proposed technique for several scenarios.

The microgrid protection proposed by Haron *et al.* (2013) is about coordination of relays using overcurrent, directional and differential techniques. The authors cite fault current levels variation, bi-directional fault current, and microgrid operation modes changes. Although the idea brings benefits for microgrid protection, the differential element used as a backup protection in case of miscoordination between overcurrent and a directional protective elements for eventual blinding and false tripping scenarios turn the system complex and expensive.

In turn, the protective scheme presented by Ustun & Khan (2015) used the differential element for high-risk zones together with an adaptive low cost communication load scheme for less critical scenarios. Nevertheless, the threshold for switching between these two strategies depends on the actual operation conditions which could constantly change.

On the other hand, a novel protection scheme based on the pre-fault and post-fault current amplitude differences is formulated by Lin Xiao Ma (2021). The results show that the protection can prevent the risk of maloperation in several external fault scenarios and identify sensitive internal faults. This paper considers the source-effect of induction motors for load branches, which for the passive unmeasurable load branch, the current amplitude difference is greater than its original value under internal faults while smaller under external faults. Also, the simulation is tested with a strong grid without connection of DG and weak grid with connection of DG.

Nevertheless, the differential impedance concept introduced by Huang *et al.* (2014) performs the protection coordination of feeders in a radial microgrid, which also can be used as backup protection or for single-ended lines. The paper shows that this method is able to clear faults in different operation modes, although for the effectiveness of the protection scheme the response depends on the precision of the parameters of the whole microgrid. Alternatively, the impedance angle-based algorithm proposed by Dubey & Jena (2021) discriminated the faults tested on IEEE 13-bus system, needing an advanced communication infrastructure for feasibility.

With another approach, a differential frequency-based on off-nominal frequency current injections was tested on islanded microgrids by Soleimanisardoo *et al.* (2019). The function in this paper was constructed from the observation that the frequency components of the currents measured at two terminals of a distribution line are different in case of fault conditions. A potential drawback of having only one inverter-based DG injecting a non-standard frequency is that if this particular inverter becomes disconnected, the suggested protection system may be unable to identify the fault. In addition, this method is limited to off-grid operation.

The relaying algorithm proposed by Zhou *et al.* (2022a) consists of adjusting the

restraint current in differential protection by utilizing the current amplitude ratio on both ends of the protected feeder. This adaptive modification aims to mitigate the impact of time synchronization errors caused by the fault data self-synchronization algorithm, thereby enhancing the performance of current differential protection. Employing a fault data self-synchronization algorithm for constructing current differential protection offers cost savings in terms of protection and communication. However, the asynchronous initiation of relays on both ends can lead to time synchronization errors, impacting the reliability of protection. In the same year, Zhou *et al.* (2022b) describes differential protection suitable for active distribution networks with complex operating modes and multiple types of DGs. The paper proposed an algorithm that uses the current zero-crossing time and current slope polarity to estimate the starting delay difference at both terminals and its advantage does not require additional synchronization equipment and high communication bandwidth. Its disadvantage is related to some factors such as noise, sampling frequency, and fault time affected the synchronization accuracy, i.e., it needs to be used in conjunction with an additional communication reliability detection method. In turn, Zhou *et al.* (2023) proposed a method based on mathematical morphology to solve synchronization accuracy and anti-noise ability. In this paper the authors proposed a solution for synchronization without additional synchronization equipment, thus greatly reducing the cost, but still fails when the effect of different fault inception angles is around 180° when the time synchronization error is relatively large.

About synchronization, Jin *et al.* (2023) introduces the difficulty to be satisfying differential protection based on the current communication conditions of active distribution networks. The extraction of fundamental frequency components is mainly challenged by distortion, frequency offset, and the instability inherent in fault currents. The suggested scheme transmits only computational outcomes rather than sampled values, thereby successfully preventing any adverse effects from arising from data synchronization errors.

Nonetheless, the proposal of El-Sayed *et al.* (2021) is an statistical algorithm which extracts features of the differential quantities from the interharmonic components of

currents and voltages signals. The proposed current limiter performs an amplitude modulation of the output fault current from the inverter. This method requires minimal bandwidth communication to detect and isolate the fault. Although the proposed strategy has been validated, the method is capable of protecting only islanded microgrids like former example.

Anudeep & Nayak (2022) also used differential features to construct a decision tree-based data-mining model where the training time could be higher than the testing time. Furthermore, the transient period information after fault inception was used in a differential features-based protection scheme based on spectral energy content complemented by an estimation of a phasor deviation of the current signals. This concept was already used by Aghdam *et al.* (2019) which implement a wavelet transform-based differential faulty energy, considering DG stability, from the zero-sequence current to identify high-resistance faults in active distribution networks, but rapid fault elimination is achieved only if lateral fuses are coordinated with agents.

On the other hand, a recent proposal focused on the time synchronization error of the differential protection schemes in active distribution networks by adaptively modifying the restraint current considering the current amplitude ratio on both terminal CTs (dos Reis *et al.*, 2021). It can be concluded that the proposed multi-agent architecture is a viable solution, despite the approach used a more sophisticated infrastructure with means that is a significant cost associated with its communication system.In order to minimize the cost of data synchronization, Miao *et al.* (2023) proposes an innovative differential protection scheme based on an extended dynamic time warping distance. The scheme promises to work reliably under various fault locations and fault resistances, but fails when the data synchronization reaches 36° and the transition resistance reaches 60 Ω. Furthermore, frequent adjustment of the protection limit must be avoided when disturbances occur.

Moreover, the protection scheme proposed by Nsengiyaremye *et al.* (2020) introduce a low-cost communication differential element and it is motivated by the limitations of overcurrent and distance relays in microgrid. The article based differential protection by comparing binary state outputs of relays at both ends of the line thus requiring

a simple, flexible and low bandwidth communication system. However, it has been shown that careful consideration is essential when selecting the differential protection parameter, as traditional differential current relays may lose effectiveness in scenarios with high inverter penetration. This is due the impact of the variance between the sequence components of the fault currents on each side of the line.

One of the recent works related to differential protection is an application focused not on current, but on voltage-based relay by Manditereza & Bansal (2020). This paper suggests that the relay algorithm accomplishes its protective role by performing calculations on active power differentials and sensitivity, depended on voltage measurements within a designated protection zone. Although the operation of the proposed scheme is efficient and selective, it must be highlighted that all of the differential protection proposals seen so far require a CT in each line terminal and another in DGs feeders, which makes the system expensive when adding more CTs.

The paper of Chen *et al.* (2020) presents a differential impedance protection algorithm which uses as quantities a differential impedance and restraint impedance in different operating states such as normal operation, external faults and internal faults. In addition, it is pointed out that an additional criterion is formulated using the amplitude characteristic of the fault current to address potential dead zone faults. Despite its contribution, the technique experiences difficulties to deal with high resistance ground fault, i.e., the performance of the proposed method is not satisfactory when the fault resistance is greater than 300 Ω.

Moreover, a coordinated multi-element current differential is discussed in Nikolaidis *et al.* (2022). The authors present a current differential protection scheme that uses a ring topology to test a differential element against faults with a critical value of fault resistance, while an instantaneous differential element is activated against the most severe faults. The applicability of the proposed scheme does not take into account the optimal number of differential relays. Also, a limitation described in this article itself is that the supply or intermediate load of the DG on the performance of the differential protection is not addressed.

In contrast to current protection methods, Liu *et al.* (2022) suggested that its

transients-based relaying technique has a significant advantage by demonstrating substantial resilience to variations in system fault levels, fault types and locations, microgrid operating conditions, and the control strategies implemented on the inverters. In addition, it has a significantly reduced sampling frequency requirement compared to traveling wave-based methods. This study did not consider a self-learning based threshold setting (adaptive technique), and the network uses several CTs (two between two busbars), which increases the cost of implementation.

Dua *et al.* (2023) presents a protection scheme based on the differential angle of the positive sequence superimposed current, using only the positive sequence current phasor from both ends of the line. The method collects current phasor readings from low-cost microphasor measurement units. In addition, real-time hardware-in-loop testing is performed to enhance the verification of the scheme for practical application. However, it is only effective when the fault current is at least 10% of the nominal value.

The data mining models for fault detection and classification, which are based on deep neural networks, are constructed using datasets of differential current phasors. These datasets are generated under different fault and operating conditions within the microgrid. The variations include different fault types, changes in fault location, fault resistance, distributed generation penetration in both grid-connected and islanded operating modes, and different types of DG units verified by Samal *et al.* (2023). This scheme also does not consider the influence of the sporadic and unpredictable characteristics of distributed generation on the protection method.

Tables 2.1 , 2.2 and 2.3 summarize the entire literature review and compare it with the proposed algorithm. In table 2.1, it can be seen within the works that use differential protection, the basic concept used to employ this type of protection, as well as the mode of operation applied, on-grid and off-grid, and the topology utilized in the network, radial or ring.

Table 2.1. Summary of Research Works - Mode Operation and Topology.

Reference	Basis Concept	Mode		Topology of Grid	
		On-grid	Off-grid	Ring	Radial
Haron *et al.* (2013)	Coordination	✓	✓		✓
Ustun & Khan (2015)	Bit error rate of the communications	✓	✓		✓
Lin Xiao Ma (2021)	Current amplitude	✓			✓
Huang *et al.* (2014)	Impedance	✓	✓		✓
Soleimanisardoo *et al.* (2019)	Current frequency		✓		✓
Dubey & Jena (2021)	Impedance	✓			✓
Zhou *et al.* (2022a)	Current amplitude	✓			✓
Zhou *et al.* (2022b)	Current polarity	✓			✓
Zhou *et al.* (2023)	Mathematical morphology	✓			✓
Jin *et al.* (2023)	Current waveform	✓			✓
El-Sayed *et al.* (2021)	Current and interharmonic		✓		✓
Anudeep & Nayak (2022)	Differential power	✓	✓		✓
Aghdam *et al.* (2019)	Tripping time differential	✓	✓	✓	
dos Reis *et al.* (2021)	Current magnitude	✓	✓		✓
Miao *et al.* (2023)	Dynamic time warping	✓		✓	✓
Nsengiyaremye *et al.* (2020)	Current	✓		✓	
Manditereza & Bansal (2020)	Voltage-based	✓	✓	✓	✓
Li *et al.* (2019)	Backup strategy	✓		✓	
Chen *et al.* (2020)	Impedance	✓			✓
Nikolaidis *et al.* (2022)	Multiple differential elements	✓		✓	
Liu *et al.* (2022)	Transient wavelet energy	✓	✓		✓
Dua *et al.* (2023)	Current differential angle based	✓	✓		✓
Samal *et al.* (2023)	Current signals	✓	✓	✓	✓
Proposed Algorithm	Current	✓	✓	✓	✓

Following the literature review found, table 2.2 shows the works that use differential protection using the traditional form of protection with two current transformers at the beginning and end of each distribution line, as well as a current transformer at the output of the DGs and one for the loads. None of the work found sought to reduce project costs by reducing the number of current transformers in the network, except for the proposed algorithm.

Table 2.2. Summary of Research Works - Number of CTs.

Reference	Basis Concept	Number of CTs		
		2 between feeder/lines	1 between load and DG	1 per zone and DG
Haron *et al.* (2013)	Coordination	✓		
Ustun & Khan (2015)	Bit error rate of the communications	✓	✓	
Lin Xiao Ma (2021)	Current amplitude	✓		
Huang *et al.* (2014)	Impedance	✓	✓	
Soleimanisardoo *et al.* (2019)	Current frequency	✓		
Dubey & Jena (2021)	Impedance	✓		
Zhou *et al.* (2022a)	Current amplitude	✓		
Zhou *et al.* (2022b)	Current polarity	✓		
Zhou *et al.* (2023)	Mathematical morphology	✓		
Jin *et al.* (2023)	Current waveform	✓		
El-Sayed *et al.* (2021)	Current and interharmonic	✓		
Anudeep & Nayak (2022)	Differential power	✓	✓	
Aghdam *et al.* (2019)	Tripping time differential	✓		
dos Reis *et al.* (2021)	Current magnitude	✓	✓	
Miao *et al.* (2023)	Dynamic time warping	✓		
Nsengiyaremye *et al.* (2020)	Current	✓		
Manditereza & Bansal (2020)	Voltage-based	✓	✓	
Li *et al.* (2019)	Backup strategy	✓		
Chen *et al.* (2020)	Impedance	✓		
Nikolaidis *et al.* (2022)	Multiple differential elements	✓		
Liu *et al.* (2022)	Transient wavelet energy	✓	✓	
Dua *et al.* (2023)	Current differential angle based	✓		
Samal *et al.* (2023)	Current signals	✓	✓	
Proposed Algorithm	Current			✓

Finally, the summary table 2.3 shows the highest fault resistance parameters tested in the proposed method, as well as the shortest tripping time for opening the circuit breaker and the load range of the proposed system.

Table 2.3. Summary of Research Works - Fault Resistance, Tripping and Loads.

Reference	Max.fault resistance tested	Max.tripping time	Range of loads
Haron *et al.* (2013)	×	152 ms	×
Ustun & Khan (2015)	×	40 ms	×
Lin Xiao Ma (2021)	100 Ω	500 ms	0.25 MW to 0.5 MW
Huang *et al.* (2014)	100 Ω	900 s	400 kVA to 0.1 MVA
Soleimanisardoo *et al.* (2019)	×	100 ms	1 MVA to 2 MVA
Dubey & Jena (2021)	1000 Ω	27.082 ms	442.296 kVA
Zhou *et al.* (2022a)	60 Ω	60 ms	(10 + j0.2) MVA
Zhou *et al.* (2022b)	60 Ω	10 ms	4 MVA
Zhou *et al.* (2023)	30 Ω	60 ms	1 MVA to 7 MVA
Jin *et al.* (2023)	30 Ω	20 ms	3.5 MVA
El-Sayed *et al.* (2021)	40 Ω	46 ms	1.2 MVA
Anudeep & Nayak (2022)	100 Ω	10 ms	×
Aghdam *et al.* (2019)	×	170 ms	×
dos Reis *et al.* (2021)	×	942 ms	5.26 MVA to 15.21 MVA
Miao *et al.* (2023)	60 Ω	20 ms	3 MW to 5 MW
Nsengiyaremye *et al.* (2020)	100 Ω	41.3 ms	0.2 MW to 1.3MW
Manditereza & Bansal (2020)	330 Ω	60 ms	×
Li *et al.* (2019)	×	195 ms	×
Chen *et al.* (2020)	100 Ω	42.5 ms	×
Nikolaidis *et al.* (2022)	8 Ω	2.786 ms	15.93MVA
Liu *et al.* (2022)	10 Ω	80 ms	20 kVA to 30 kVA
Dua *et al.* (2023)	500 Ω	0.21 ms	×
Samal *et al.* (2023)	200 Ω	242,6 ms	1.4 MW
Proposed Algorithm	50 Ω	4,4 ms	2 MW to 3.5 MW

This summary of works that used differential protection of microgrids, shows that this concept could be used more often with some treatment specific in order to implement a bus protection algorithm.

CHAPTER 3

THEORETICAL BACKGROUND

This chapter initially presents the theoretical background of the conventional differential current-based protection function. Here the operation principle and the main settings are mentioned. Also, a description of the operation modes of the inverters is presented, as well as the control scheme of PQ and V/f modes, used in off-grid and on-grid operation, respectively.

3.1 CONVENTIONAL DIFFERENTIAL PROTECTION

Differential Protection is one of the most used method for lines, busbars and transformers protection. This method establishes that the sum of all currents in one zone is zero in normal conditions, and it fastly increases in case of a short-circuit. On the other hand, a protection scheme based on this principle does not require voltage measurements and is not sensitive to power swings, sudden load changes, and voltage variations (USTUN *et al.*, 2013). The phase-segregated current-based differential protection uses the secondary currents of terminal CTs of, for example, a distribution line, as illustrated in Fig. 3.1.a. These measurements are the input signals in the protective equipment, where a previous signal processing stage is performed before being used by the relaying algorithm. The ouput signal is a trip command to the terminal circuit breakers to isolate the fault.

Internally, two quantities are determined, the operation current and the restraint current. The operation current, I_{OP}, increases when a fault occurs and it is compared with the restraint current, I_{RES}, which is typically multiplied by a percentage value, called as slope. There is several ways to calculate I_{OP} and I_{RES}, but the Figure Fig. 3.1.a. focuses in one of them. Also, it must be mentioned that this protective function

can be implemented in the phasor domain, where a phasor estimation process is performed. Alternatively, the samples can be directly used to implement the algorithm in time domain. In this work, the proposed technique uses the phasor approach, where the plane I_{OP} and I_{RES} are used. Here, the initial I_{OP} is ideally zero so it is located on the restraint zone, and it enters the operation zone when the fault occurs. Conventionally, it is imposed that this condition must remain for a quarter-cycle to confirm the presence of the fault, because this is typically the minimum time before CT saturation.

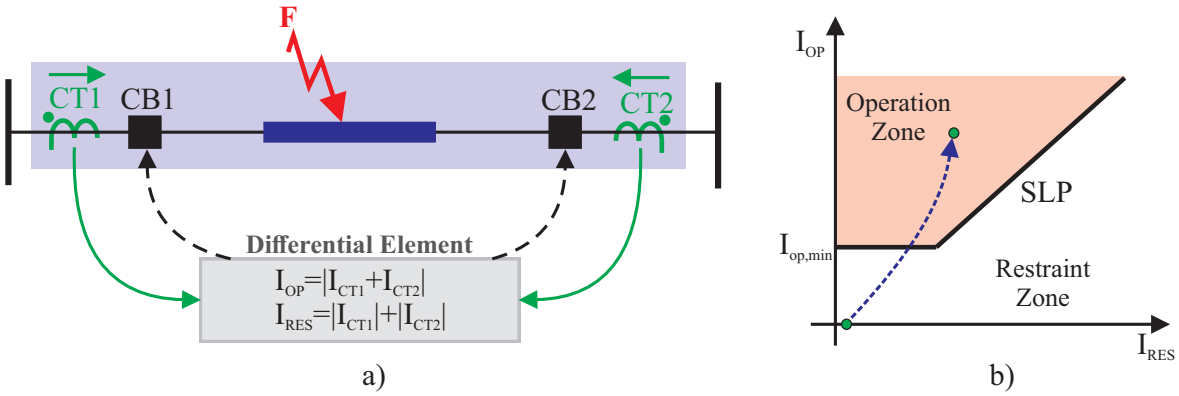

Figure 3.1. Traditional Differential Current Protection Scheme.

In differential protection, limits are used to ensure the security of the operation of the relays. In this way, measurement errors due to the saturation of the CTs, CTs ratio incompatibilities, and leaking load currents (IEEE, 2021) must be compensated to avoid malfunctions due to incorrect differential currents. In that sense ,a minimum operation current, $I_{OP,MIN}$, must be set. Normally, this value is constant and it is not dynamically modified. This current is calculated from local parameters and increases with increasing current to deal with higher measurement errors I_{min} (USTUN *et al.*, 2013).

Moreover, an additional warning element is used to sensitize a disturbance in the grid. This disturbance detector can be mathematically defined from the variation rate of the restraint current, as the Equation 3.1. If the index ΔI_{res} becomes higher than a pickup, the disturbance detector flag is activated so the protection element itself is ready to operate in case the fault conditions be recognized.

$$\Delta I_{res} = \frac{I_{res}(k) - I_{res}(k-1)}{dt}. \tag{3.1}$$

The differential current protection becomes interesting in microgrids because of its capability to be selective, sensitive, and fast. The challenges of this type of protection refer to the need for digital relay communication and the associated cost, which implies the use of relays and CTs on each line terminal and others on the DG feeders (RODRIGUES, 2017).

3.2 CONTROL OF THREE-PHASE INVERTERS

The devices commonly recognized as inverters, which convert direct current (DC) to alternating current (AC), are categorized as either current source inverters or voltage sources, based on topology of the power circuit and corresponding the nature of the power supply source. Inverters are engineered to send power back to the grid and encompass several tasks typically carried out by protection relays, such as synchronization, voltage regulation (both over and under), and frequency monitoring.

There are different types of requirements when it comes to microgrid control depending on the DGs mode of operation. The basis and difficulty of discovering the best way of operating and configuring the microgrid implies analyzing the output characteristics of the DG through different control methods and its failure characteristics within the microgrid under different operational strategies. A microgrid controller needs to be sufficiently resilient to handle intermittence of generation and loads within the microgrid, stemming from factors such as shifts between grid-connected and islanded modes, power balance fluctuations, changes in configuration, and potential communication breakdowns, particularly if the controller depends on signal communication (FARINA, 2018).

There are three major control strategies for inverters in the literature: Grid feeding (PQ control); Grid forming (V/F control) and Grid supporting (droop control).

- The grid-feeding power converters can be represented by current sources and they receive as input reference the power that they must deliver. These converters are well-suited for parallel operation with other grid-feeding power converters in grid-connected mode. Typically, the converters are connected to intermittent

renewable sources so the main concern is to extract the maximum power from the resource, i.e., wind or solar, by implement the Maximum Power Point Tracking algorithm (MPPT) on the rectifier stage. On the other hand, the reactive power typically is zero. In this operation mode, PQ, the converter uses the voltage and frequency of the grid to implement the control loop.

- The grid-forming power converters of closed-loop control ensures they function as ideal AC voltage sources, characterized by a specified amplitude and frequency. These converters act as low-output impedance voltage sources, requiring a highly precise synchronization system to operate seamlessly alongside other grid-forming converters in parallel. This is equivalent to the V/f operation mode because the converters in this condition regulates the network voltage and frequency. This operation mode is used when the inverter is in off-grid operation because it is necessary to define a reference for the others converters.

- The grid supporting power converter is designed for manager either as a voltage source with a series impedance or as a current source with a parallel impedance. Regardless of the configuration, its primary goal is to contribute to the regulation of the AC grid voltage amplitude and frequency by overseeing the control of active and reactive power supplied to the grid (ROCABERT *et al.*, 2012). These type of operation is similar to the droop control used for synchronous machines where the there is a relation between the active power and the frequency, and another relation between the voltage and the reactive power. Basically, this approach defines the way to dynamically share the load by following the droop characteristic, but keeping the nominal frequency. Analogously, the sharing of reactive power can be performed together with the voltage regulation (KHAN *et al.*, 2019).

3.2.1 PQ MODE

The PQ control oversees and regulates the active power generated and used within the microgrid. Power generation, load requirements, and energy storage are adjusted by

it to ensure a harmonized distribution of active power based on the system's demands. Alongside managing active power, the PQ control also oversees reactive power in the microgrid, which is important for maintaining voltage quality and avoiding problems like stability and preventing issues such as voltage fluctuations and excessive network losses. It can intervene to either supply or absorb reactive power as needed to uphold system integrity. Furthermore, the PQ control generation, load, and energy adjustment to maintain voltage levels within acceptable parameters across all microgrid points. This is crucial to ensure the secure operation of electrical equipment's and ensure the quality of service for users.

In this case, the active power to be delivered from the inverter can be defined by the Maximum Power Point Tracking (MPPT) algorithm. On the other hand, the reference to reactive power is commonly imposed to be zero. Based on that, the phase of voltages signals is firstly captured by the Phase Locked Loop (PLL) and it is incorporated into the grid currents and voltages signals in the dq reference, as shown in Fig. 3.2. From that, the calculated powers PQ are compared with their corresponding references and the error passes through PI controllers. The output is the current references idq which are now compared with the measured idq. The PI control applied on these errors provides the voltage references, vdq,ref , which are the reference voltages to be used by the inverter with a previous inverse transformation dq to abc.

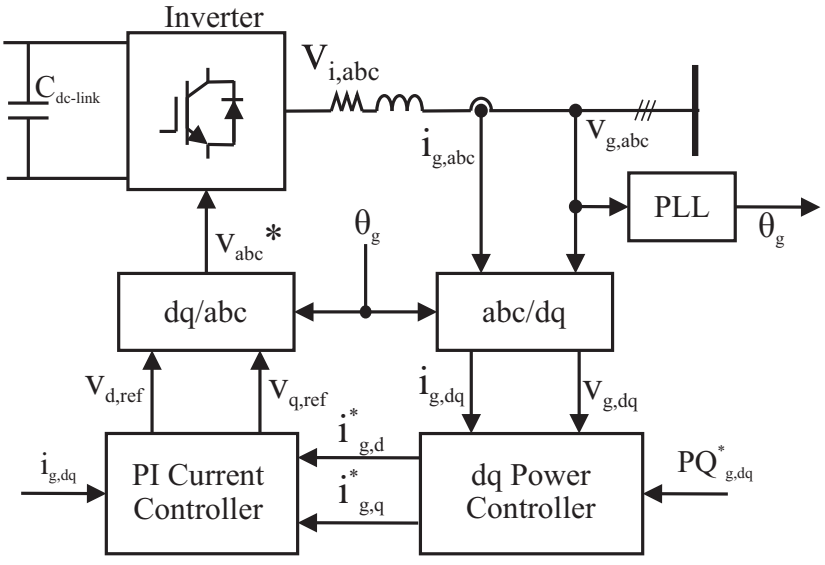

Figure 3.2. On-grid PQ mode

3.2.2 V/F MODE

The V/f control monitors and controls the frequency of electricity in the microgrid. It adjusts power generation and load to keep the frequency within specified limits, thus ensuring system stability. Changes in frequency can indicate imbalances between generation and load, and V/f control acts to correct these deviations. As with PQ control, V/f control also regulates the voltage in the microgrid to keep it within the appropriate limits. This is crucial for ensuring the safe operation of electrical equipment and the quality of the energy supply to users. In this condition, the main concern is to provide electric energy to the local load with the nominal voltage and frequency. Thus, the voltages and currents at the supplying point to the load are transformed into dq frame to calculate the actual dq powers, PQ. These values are then used as inputs in the droop controller to define the corresponding voltage and frequency based on the droop characteristic, Vdroop,ref and Fdroop,ref , as shown in Fig.3.3. Now, they are compared with the nominal voltage and frequency of the system to define idq,ref through a PI controller. The error between these quantities and the actual idq is reduced with a second PI controller so the obtained vdq,ref is used by the inverter in a similar way to PQ mode control.

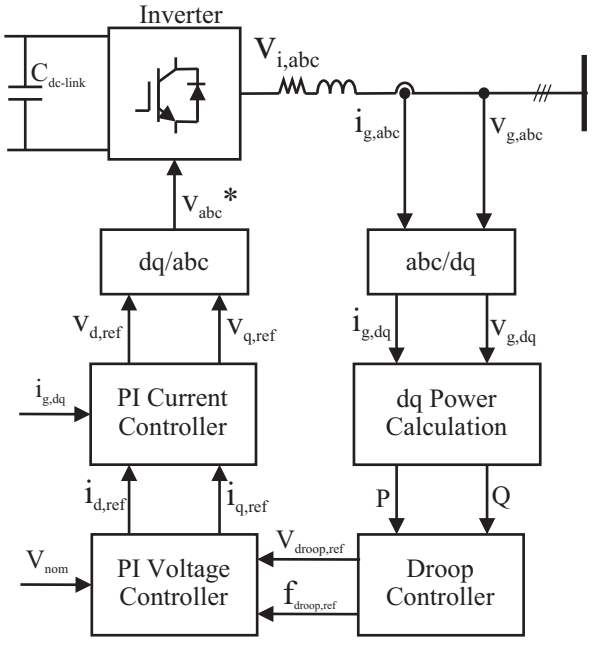

Figure 3.3. Off-grid V/f mode.

CHAPTER 4

PROPOSED PROTECTION FUNCTION

In this chapter, the proposed technique is described. The protection scheme and the necessary equipments are mentioned, and thereafter the algorithm itself is detailed. Here, the main protection logic and a backup logic for dead zones are described.

4.1 PROPOSED PROTECTION SYSTEM

In order to explain the proposed algorithm, the Figure 4.1 illustrates a part of a microgrid where a inverter-based generation unit is connected to a line of a microgrid through a circuit breaker. In this figure, distribution lines, DL1 and DL2, are connected to a common busbar where a load, denoted as L2, is connected. A distributed generation unit, DG1, is the main responsible for supplying power to the load L1. Current transformers, CT1 and CT2, are installed at the beginning of DL1 and DL2, respectively, and these lines can be opened using the circuit breaker pairs CB1-CB2 and CB3-CB4, respectively. Furthermore, DG1 is equipped with its own current transformer, denoted as CTDG1, and a dedicated circuit breaker, CBDG1.

Unlike the conventional differential protection scheme, where an additional current transformer would be typically positioned on the right side of DL1, in this proposed scheme, CT2 is used for this purpose, as depicted in Figure 4.1. This deviation from the conventional arrangement is made to accommodate the specific requirements and configurations of the microgrid model being developed.

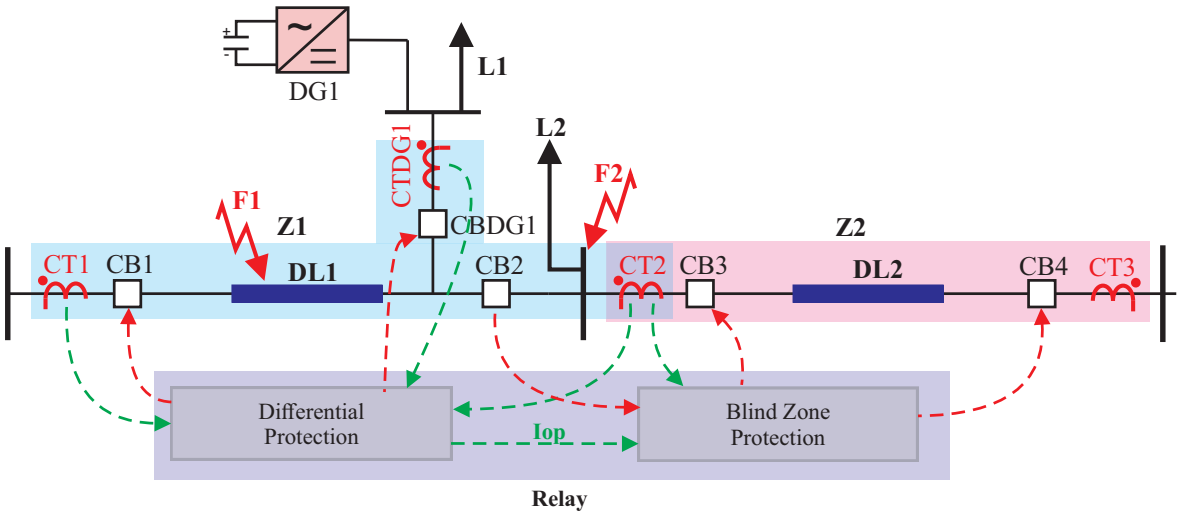

Figure 4.1. Proposed Scheme

In this way, the operation and restraint currents calculation uses the secondary signals of CT1, CT2 and CTDG1, and they can be mathematically determined, respectively, as:

$$I_{op} = |I_{CT1} - I_{CT2} + I_{CTDG1}|, I_{res} = |I_{CT1}| + |I_{CT2}| + |I_{CTDG1}| \tag{4.1}$$

Based on these calculations, the trip command to circuit breakers CB1, CB2, and CBDG1 is sent if the conditions of Eq. 4.1 are satisfied. In turn, DG1 keeps supplying the load L1 if the illustrated topology is adopted. On the other side, the circuit breakers, CB3 and CB4, remain closed so the load L2 will be supplied by downstream sources. Nevertheless, the opening of these specific CBs will eliminate the fault when it occurs within the physical protection zone of DL1, delimited by these CBs, such as the fault F1 in Fig. 3. Moreover, it is possible to identify that there is a dead zone, for example, between CB2 and CT2, so a complementary logic is necessary to overcome this issue and eliminate the fault F2. This additional function can use the logic state of the opened CBs as input and verify if the trip conditions of the differential function are still satisfied in Z1. Then, the output of this backup element is a trip command for CB3 and CB4.

4.1.1 Main Protection Logic Description

Initially, it is confirmed whether the internal fault conditions described in Eq. 4.2 of the differential element are known, indicating the logic state of SFI = 1, as illustrated in Figure 4.2.

Traditionally, these conditions should be fulfilled within a quarter cycle, which represents the minimum time required for CT saturation. However, the presence of contributions from Distributed Generators in healthy zones may sensitize the protection element of their respective zones. Therefore, to enhance the overall security of the microgrid protection scheme, an incremental operation current for each protection zone, denoted as ΔIop, is utilized to prevent incorrect operations. This incremental current can be calculated as follows:

$$\Delta I_{op} = I_{op}(k) - I_{op}(k - N) \tag{4.2}$$

To trigger relay operation, the incremental operation current ΔI_{op} needs to exceed a predefined minimum threshold, denoted as $\Delta Imin$. Additionally, the ratio between ΔIop values of zones where $S_{FI} = 1$ is computed. Subsequently, it is ensured that the index of the faulted zone is at least λ times greater than that of the other zones. The lambda value was established in accordance with a specific margin to differentiate between faulty and non-faulty zones. This value should not be very low, as this could lead to more than one faulty zone being misrecognized, and it should not be very high, as this could lead to delays in the operation. Following this verification process, the trip command is issued to the circuit breakers (CBs) if both the conditions of the differential and incremental elements are met, as illustrated in Figure 4.2.

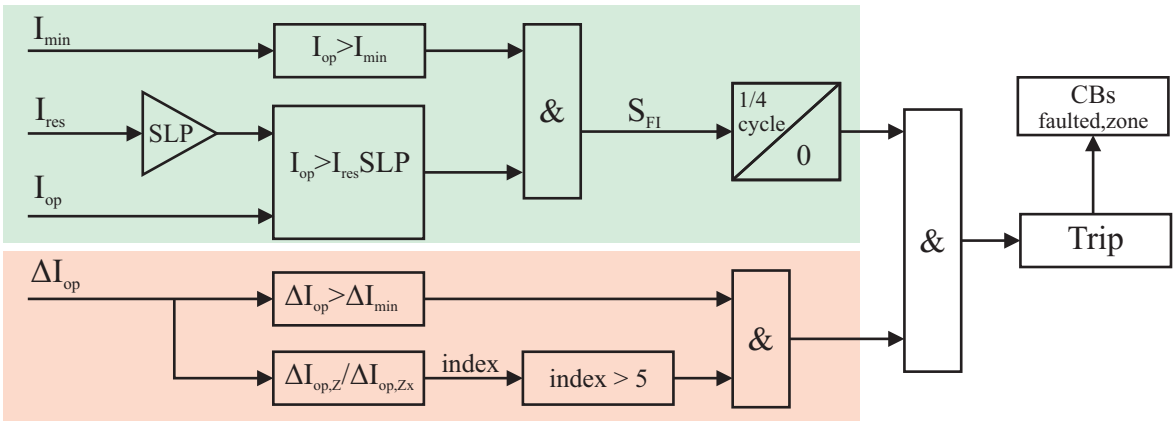

Figure 4.2. Main protection logic of the proposed algorithm.

4.1.2 Adaptive Minimum Threshold Logic

An additional strategy was incorporated to dynamically define the minimum pick-up to suitably deal with the generation-load changes. This intelligent system automatically adjusts the minimum value of the operation current based on dynamic conditions. This specific algorithm is necessary because load feeders do not have a exclusive current transformer for this measurement and this current is not considered for calculation of I_{OP} and I_{RES}.

Adaptive Minimum Threshold Logic is a strategy which uses the balance generation-load as a factor for the definition of its value. The adaptive logic can be executed through the utilization of control and machine learning algorithms, which consider real-time data such as the microgrid's current demand, the capacity of distributed energy sources like solar panels and wind turbines, the accessibility of energy storage options such as batteries or other storage systems, and the charging status of devices linked to the microgrid.

The process of adapting logic could involve several steps, including monitoring, data collection, real-time analysis, decision-making, adjustment of the minimum current value, and evaluation and feedback. During monitoring, sensors and meters would be employed to continually monitor the operating current of the microgrid, along with other relevant variables like voltage, frequency, and temperature. The data collected by these sensors is transmitted to a processing system where it is stored and analyzed.

Real-time control and machine learning algorithms then scrutinize the data to identify patterns, trends, and correlations among the microgrid's variables. Based on this analysis, the system would make decisions regarding the appropriate minimum operating current for the microgrid at any given moment. Subsequently, utilizing this information, the system adjusts the minimum current value to optimize the microgrid's performance and efficiency. Lastly, the microgrid's performance is continuously assessed to validate the effectiveness of the decisions made by the adaptive logic. The feedback obtained from this evaluation is utilized to enhance the system's future performance. In this approach, the decision threshold, responsible for distinguishing between desired signals and unwanted noise or interference, is constantly adapted to accommodate fluctuations in operational settings. This proves particularly advantageous in grid where signal characteristics undergo substantial variations over time, making it challenging to establish a fixed threshold that remains effective across all scenarios.

The implementation of the Adaptive Minimum Threshold Logic can take different forms, employing either signal processing algorithms or machine learning methodologies. These techniques, described in the previous paragraph, empower the system to continuously monitor the quality of signals and flexibly adjust the decision threshold to enhance detection accuracy and performance. Adapting the threshold according to channel conditions can significantly improve the robustness and reliability of the communication system, guaranteeing consistent and reliable performance when detecting events or making decisions.

Despite the explained advanced methods, in this work, this logic is simple and uses as inputs the operation current and its corresponding instantaneous incremental value which is calculated as:

$$\Delta I_{op-inst} = \frac{I_{op}(k) - I_{op}(k-N)}{\Delta t} \tag{4.3}$$

It's important to note that $\Delta I_{op-inst}$ differs from the incremental operating currents, ΔI_{op}, utilized for identifying non-faulted protection zones, which are computed with a one-cycle interval between samples. As a result, it's conceivable to establish that the minimum pickup level should be M times the operating current when there are

changes in load or generation powers, which can be discerned if $\Delta I_{op-inst}$ falls below a certain threshold. To find the value of M, previous simulations were performed to identify which value would be ideal. It was determined that 1.3 does not cause any sort of delay or inappropriate actuation. Conversely, in the event of a short-circuit, this value experiences a sudden increase, and $I_{op,min}$ should adopt the value from one cycle before the fault occurrence and remain constant thereafter.

For instance, Figure 4.3 illustrates the change in I_{min} with M = 1,3 when a load is disconnected at 0,6 s in a microgrid, followed by the connection of another load at 0,8 s. Subsequently, a short-circuit occurs at 0,9 s. It can be observed that I_{min} remains elevated compared to I_{op} following the load alterations, but its value remains constant after the occurrence of the short-circuit event, which is initially perceived as a significant disturbance due to the sudden increase in $\Delta I_{op-inst}$.

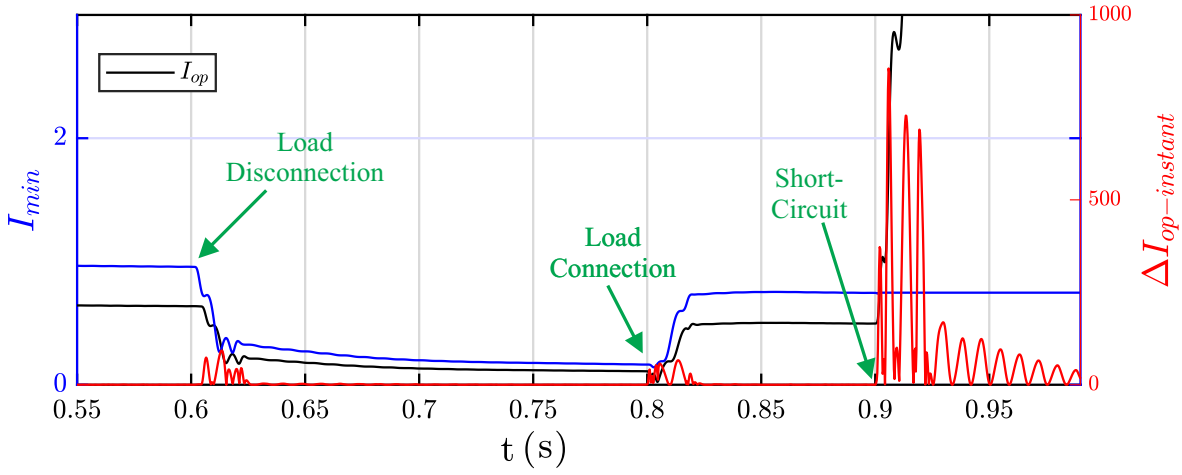

Figure 4.3. Response of the adaptive minimum pickup strategy.

4.1.3 Backup Dead Zone Protection Logic

The dead zone refers to a critical sector of the grid where the primary protection system may fail to accurately detect and isolate a fault because it is not covered by any main protection zone. Then, this backup logic serves as an extra protective layer, activating only when the primary protection mechanism is incapable of effectively addressing a fault. Its purpose is to quickly identify and isolate the fault, thereby minimizing disruptions to microgrid operations and preventing the fault from spreading to

other sections of the system.

The functionality of the backup logic in the dead zone typically involves continuous monitoring of system conditions, which includes detecting fault signals by the primary protection system. If a fault is identified but the primary protection fails to respond within a predetermined timeframe, the backup logic is triggered.

This backup logic can rely on various criteria to determine when intervention is necessary. For instance, it may take into account the continuity of fault signals or the absence of response from the primary protection devices. Once activated, the backup logic can issue commands to open circuits or disconnect specific areas of the microgrid, effectively isolating the fault and restoring system stability.

The backup logic in the dead zone proposed in this work starts by taking the instant k, when the command to trip the circuit breakers of the faulted zone is sent. Simultaneously, it continuously monitors the conditions of the internal fault, ensuring that the status indicator S_{FI} remains in the logic state 1. Furthermore, the logic also observes the operational status of the opened circuit breakers in the faulted zone, indicated by CB = 0. If these conditions persist for four cycles after the instant k, the circuit breakers of the adjacent zones are triggered to open as well, as depicted in Figure 4.4. The correct circuit breakers to be opened are defined by the protection zones.The time of four cycles is necessary to identify, according to the logic of the proposed algorithm, that the circuit breaker of the adjacent zone in which the current increased should also be opened. Thus, the increase or decrease in the incremental currents in the CTs of the adjacent zones in which the short-circuit occurred indicates that this zone must also be protected, as the short-circuit occurred in a dead zone. This action aims to contain the fault and prevent its spread to neighboring zones, thereby safeguarding the integrity of the microgrid.

In order to guarantee the selectivity of the relaying scheme and ensure accurate identification of the adjacent zone to be opened, an instantaneous overcurrent element is incorporated. This element complements the backup logic by confirming the adjacent zone based on the current magnitude measured by the common current transformer shared between the faulted zone and the adjacent one. The current measured by this

CT must exceed a predetermined minimum threshold value, denoted as $I_{CT,min}$, to confirm the need for opening the adjacent zone.

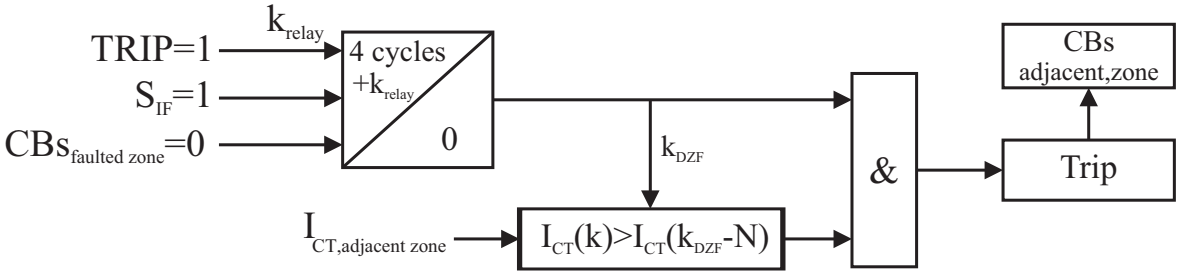

Figure 4.4. Backup logic of the proposed algorithm for dead zone protection

4.2 SIGNAL PROCESSING

In this work, in order to use differential protection in the algorithm, the analog currents obtained by the CTs are first passed through 2-order low-pass filters. In this technique, the sampled signals are filtered by low-pass filters to remove high-frequency components and obtain a smoother and more accurate representation of the original signal. Low-pass filters are designed to allow lower frequencies to pass through, while attenuating higher frequencies. This is fundamental in phasor estimation, as short-term variations in current signals can be due to noise or transients that do not reflect the long-term characteristics of the electrical system. The use of low-pass filters in phasor estimation helps to reduce the distortion effect in the estimated signals, ensuring a more faithful representation of the real conditions of the electrical system.

After passing through the low-pass filter, the current signal is discretized and re-sampled in sample/cycle quantities. The process of discretizing samples by cycles in current signals involves converting continuous analog current signals into discrete values that represent each cycle of the electrical frequency. During this procedure, samples of the current are gathered at regular intervals, typically aligning with integer multiples of the fundamental period of the electric current.

This approach proves particularly valuable in systems dedicated to monitoring and analyzing electricity, especially those operating in real time. By discretizing samples according to cycles, it becomes feasible to acquire a precise and efficient portrayal of

the periodic attributes of the current signal. This allows for thorough examinations of phenomena such as harmonic distortion, phase imbalance, and other irregularities.

Moreover, employing discretization by cycles streamlines the process of signal manipulation, as samples are organized based on the cycles of electrical frequency. Consequently, this facilitates the analysis and understanding of data, which is especially beneficial in applications involving the control and safeguarding of electrical systems, where rapid decision-making is contingent upon the state of the current signal.

The third step of the proposed algorithm is phasor estimation. Phasor estimation refers to the accurate determination of the amplitude, phase and frequency characteristics of the current signal being monitored. This is crucial for correctly identifying abnormal conditions, such as short circuits or system faults, and activating the appropriate protection devices to isolate the fault and prevent damage to electrical equipment and the whole grid.

CHAPTER 5

RESULTS AND DISCUSSION

This chapter evaluates the performance of the proposed microgrid differential protection scheme. To do this, the electrical microgrid modeled in EMTP program is firstly described. From that, different types of fault are simulated. They can be internal or external to certain protection zone, with different types of fault impedance, when the microgrid is connected and disconnected from the main grid. Also, radial and ring topologies are used to perform this assessment. In addition, faults in dead zones were also tested to demonstrate the benefits of the proposed protection scheme. In addition, a sensitivity analysis is carried out for internal and evolving faults, combining different values of fault resistance to ground and between phases. The locations of faults to be simulated to test the proposed algorithm are presented in Figure 5.2.

5.1 ELECTRICAL MICROGRID MODEL DESCRIPTION

The electrical network under consideration is composed of a main grid operating at 24,9 kV and 60Hz and four additional sources of distributed generation. These sources are represented by three-phase inverters CC/CA, denoted as DG1, DG2, DG3, and DG4. Each distributed generation unit is associated with a specific load, labeled as L1, L2, L3, L4, and L5. To enhance system reliability and functionality, the network has been divided into protection zones. Each protection zone has a current transformer with a transformation ratio of 100/5, a circuit breaker, and a distribution line. The distributed generation units, together with their respective loads, are connected to busbars, each equipped with its own circuit breaker and CT. Nonetheless, the Zone Z6 deviates from this configuration, featuring only a CT and a circuit breaker. The CTs associated with DG1 and DG3 have a transformation ratio of 200/5, distinguishing

them from the others. In addition, the system layout follows a ring network topology, which can be transformed into a radial configuration if the CB11 circuit breaker is opened. This feature reduces the grid flexibility, as depicted in Figure 5.1. The parameters used to model each of the components of the generation sources and the network are described and illustrated in figure 5.1 and summarized in table 5.1.Also, several simulations helped to define the operation modes of DGs in order to guarantee voltage and frequency stability in off-grid operation. Specifically, DG1, DG3 and DG4 adopt the V/f mode while DG2 remains in the PQ mode.

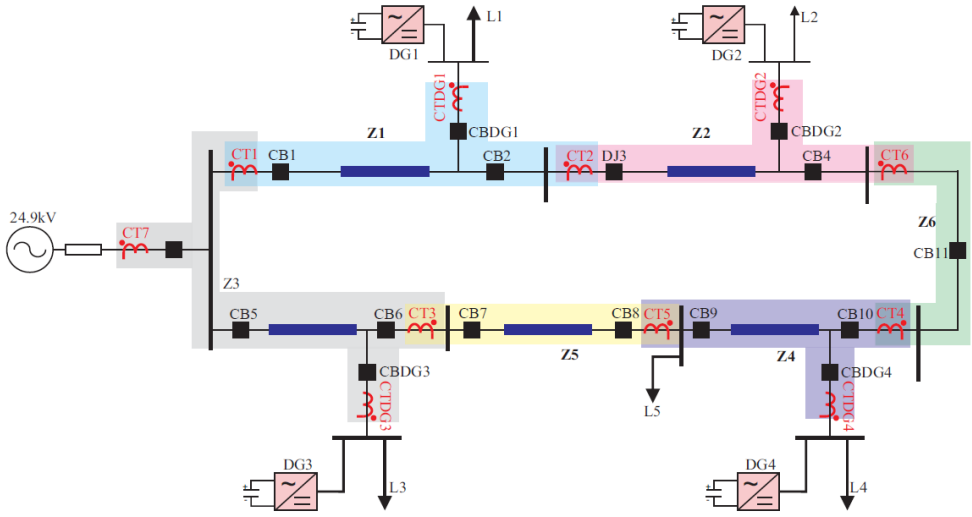

Figure 5.1. Proposed Grid System

Table 5.1. Parameters of the Simulated Power System Components

Equipment's	Parameters	
Source	Rated voltage Frequency	24,9 kV 60 Hz
DG 1	Generation Operation Mode Ongrid Operation Mode Offgrid	6 MW PQ VF
DG 2	Generation Operation Mode Ongrid Operation Mode Offgrid	2 MW PQ PQ
DG 3	Generation Operation Mode Ongrid Operation Mode Offgrid	6 MW PQ VF
DG 4	Generation Operation Mode Ongrid Operation Mode Offgrid	8 MW PQ VF

The parameters used to model each of the components of the loads are described and illustrated in figure 5.1 and summarized in table 5.2 are shown below.

Table 5.2. Parameters of the Simulated Power System Components - Loads

Equipment's	Parameters	
Load 1	Active power Reactive Power	3 MW 1 MVAr
Load 2	Active power Reactive Power	3 MW 1 MVAr
Load 3	Active power Reactive Power	2 MW 1 MVAr
Load 4	Active power Reactive Power	2 MW 1 MVAr
Load 5	Active power Reactive Power	3.5 MW 1.5 MVAr

5.2 PROTECTION ZONES

One of the main concerns of the proposed algorithm is the definition of the protection zones, which are determined by the location and logic states of circuit breakers and current transformers. In relation to the protection zones, the table 5.3 shows their composition as well as the current transformers which link them, summarizing which CT and CB are part of the protection zone. Also, the CTs in common and adjacent by protection zones are mentioned.

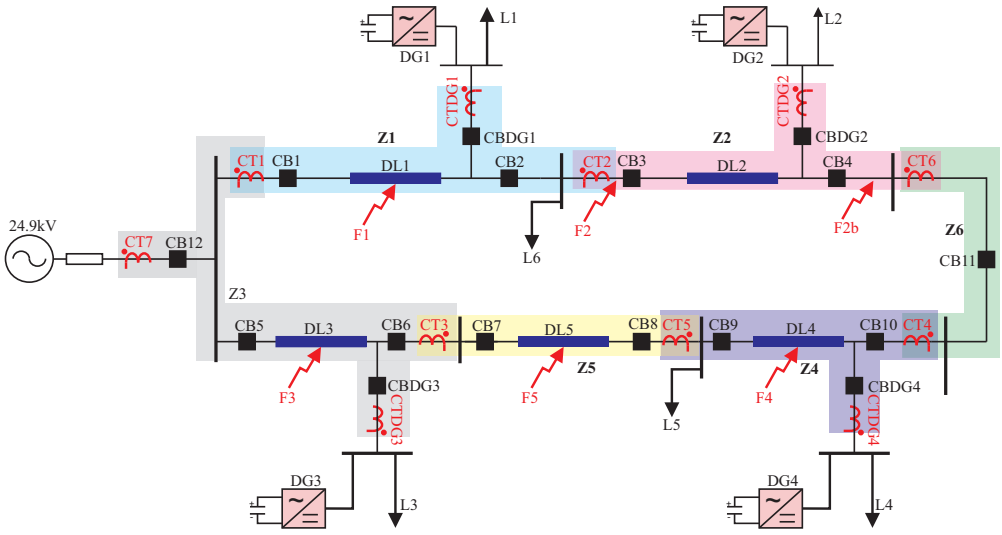

Figure 5.2. Test microgrid modeled in the software EMTP.

Table 5.3. Protection zones (CTs, CBs) and common CTs.

Zone	Equipments		Adjacent zones and common CTs					
			Z1	Z2	Z3	Z4	Z5	Z6
Z1	CTs CBs	CT1 - CT2 - CTDG1 CB1 - CB2 - CBDG1	-	CT2	CT1	-	-	-
Z2	CTs CBs	CT2 - CT6 - CTDG2 CB3 - CB4 - CBDG2	CT2	-	-	-	-	CT6
Z3	CTs CBs	CT1 - CT3 - CTDG3 - CT7 CB12 - CB5 - CB6 - CBDG3	CT1	-	-	-	CT3	-
Z4	CTs CBs	CT5 - CT4 - CTDG4 CB9 - CB10 - CBDG4	-	-	-	-	CT5	CT4
Z5	CTs CBs	CT3 - CT5 CB7 - CB8	-	-	CT3	CT5	-	-
Z6	CTs CBs	CT6 - CT4 CB11	-	CT6	-	CT4	-	-

5.3 CASE 1: PHASE-TO-PHASE FAULT (ON-GRID AND OFF-GRID OPERATION)

The first scenario is a phase-to-phase AB fault in line DL1 at 0.9 seconds, i.e., in the protection zone Z1. This case is also used to compare the effectiveness of the proposed algorithm against the conventional differential element. To achieve this, an

extra current transformer was added between CB2 and L6 with appropriate polarity adjustments for the computational implementation of the traditional approach. Initially, the fault was tested with the system isolated from the grid. In this case, the operation modes of DG1, DG3, and DG4 is V/f mode, and only DG2 operates in PQ mode. It was previously verified that these settings ensure the microgrid stability.

It can be seen in Fig. 5.3 that I_{op} in Z1 enters into the operation zone. This behavior also occurs in zone Z3 but it occurs slightly. In a conventional protection approach, it would wrongly issue the trip command to the corresponding circuit breakers. For this reason, it is very important to monitor the variation of ΔI_{op}. Specifically, the amplitude of ΔI_{op} of Z1 is much higher than the other zones, as shown in Fig. 5.4, which makes the algorithm identify that the zone where the fault occurred is Z1, and not Z3. In relation to the other zones, in no case, the operation current becomes higher than the restrain current, and the variation of ΔI_{op} is negligible. Then, it can be concluded that the protection scheme will correctly operate.

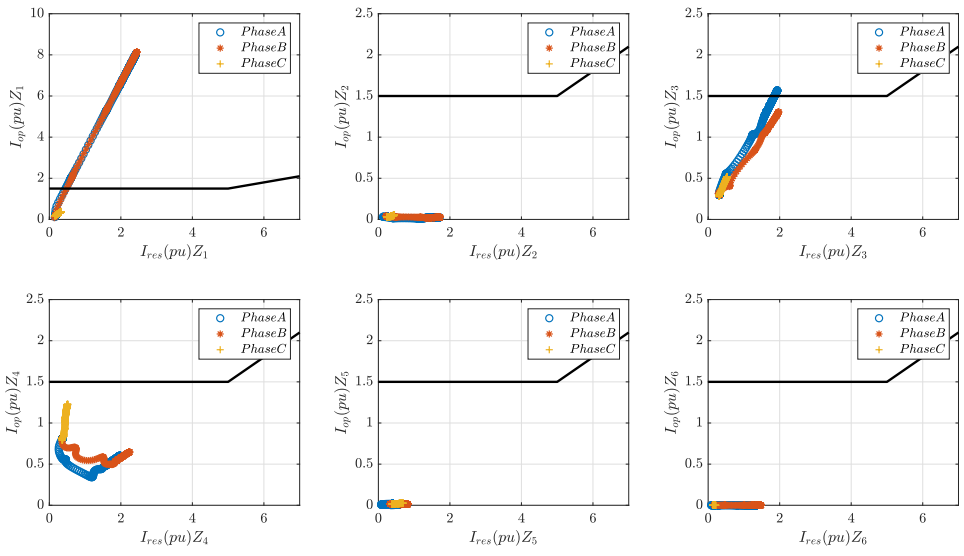

Figure 5.3. Short-circuit AB in Z1 off-grid operation: $I_{op} \times I_{res}$

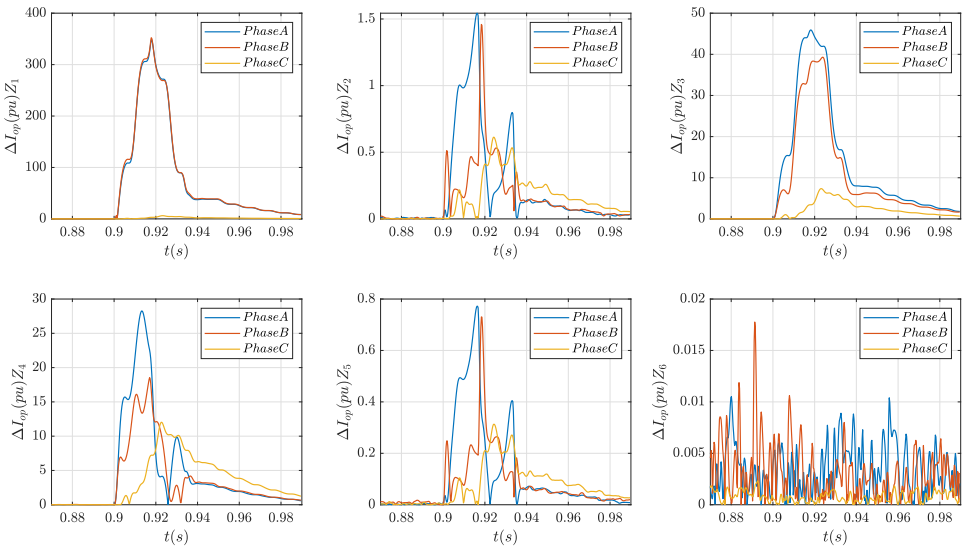

Figure 5.4. Short-circuit AB in Z1 off-grid operation: $\Delta I_{op} \times t$

Moreover, as represented in Fig. 5.5, the differential currents in the faulty phases enter the operational range as predicted. Fig. 5.6 confirms a quick trip occurrence at 0.90194 seconds, while the traditional element exhibits delayed operation at 0.90688 seconds, as illustrated in Fig. 5.7. This variance arises because the proposed scheme validates fault location by comparing incremental operation currents, whereas the traditional method necessitates a quarter-cycle delay for confirmation.

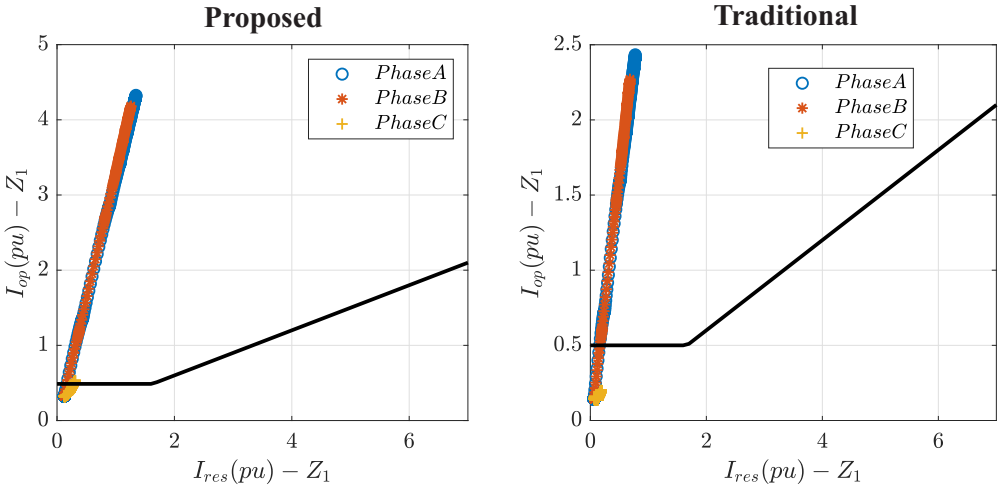

Figure 5.5. $I_{res}.SLP \times I_{op}$−Fault AB in Z1−$Off - grid$.

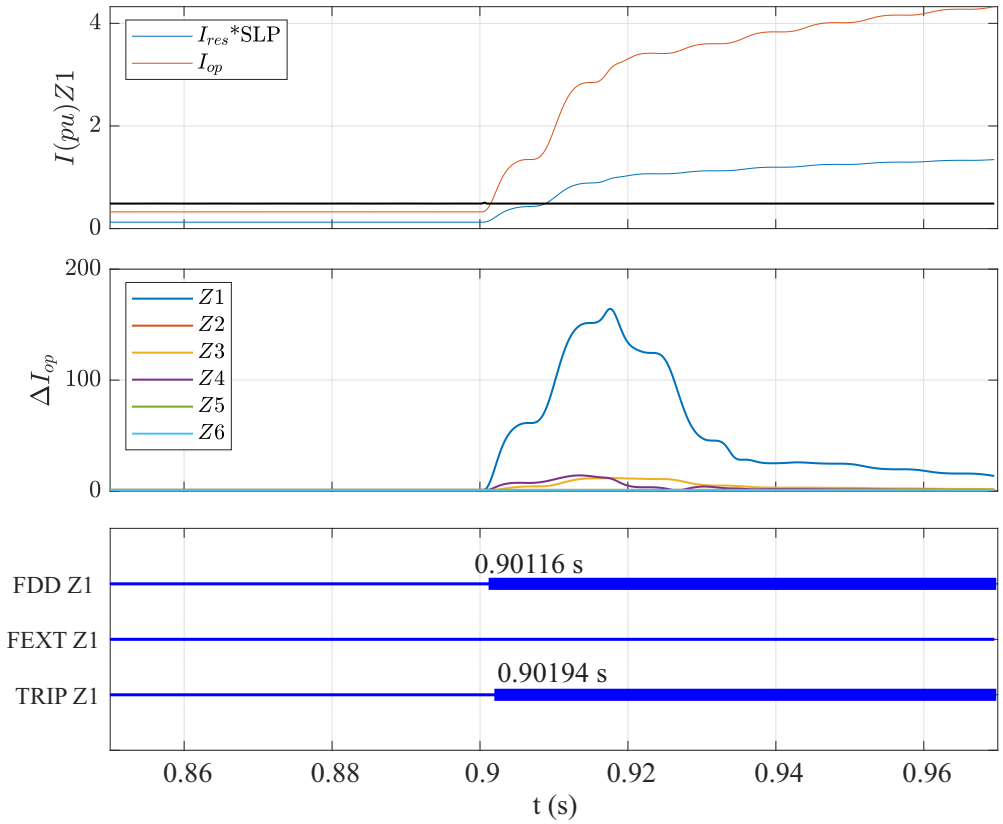

Figure 5.6. Case 01. Time domain response of the proposed function 87. Off-grid operation.

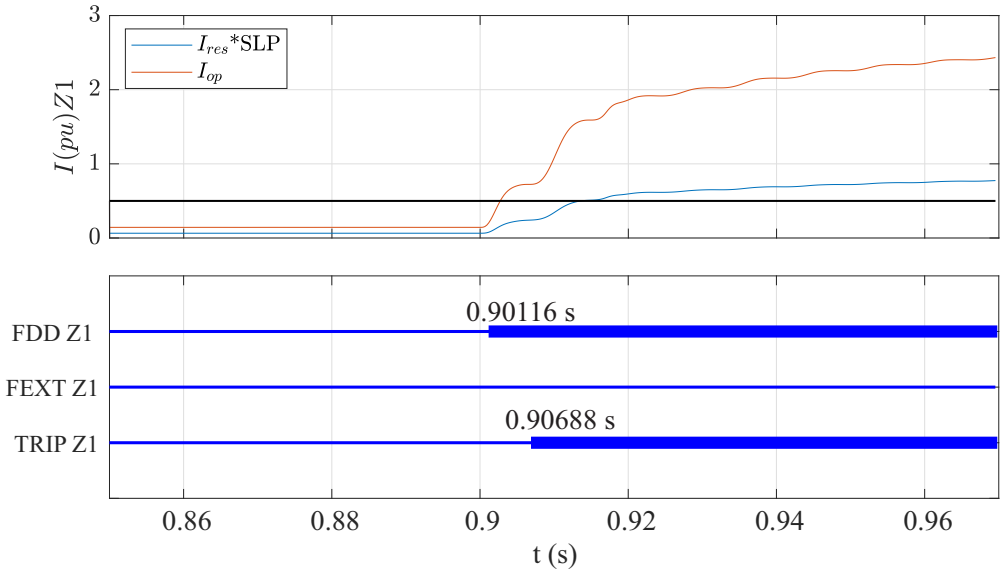

Figure 5.7. Case 01. Time domain response of the traditional function 87. Off-grid operation.

Switching to on-grid mode, differently of off-grid, it can be seen in Fig.5.8 that I_{op} in Z1 is the only one to enter into the operation zone. Figure 5.9 shows that the amplitude of ΔI_{op} of Z1 is much higher than in the other zones.

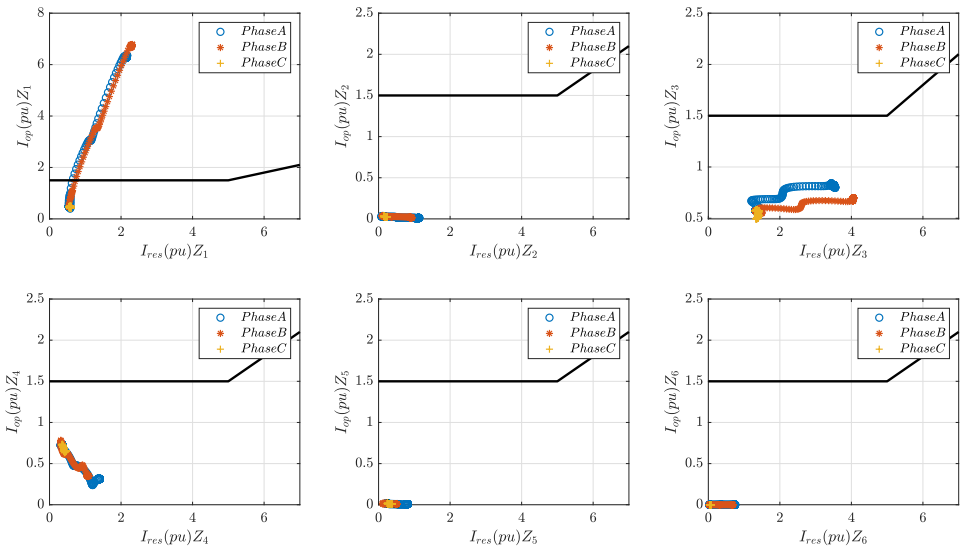

Figure 5.8. Short-circuit AB in Z1 on-grid operation: $I_{op} \times I_{res}$

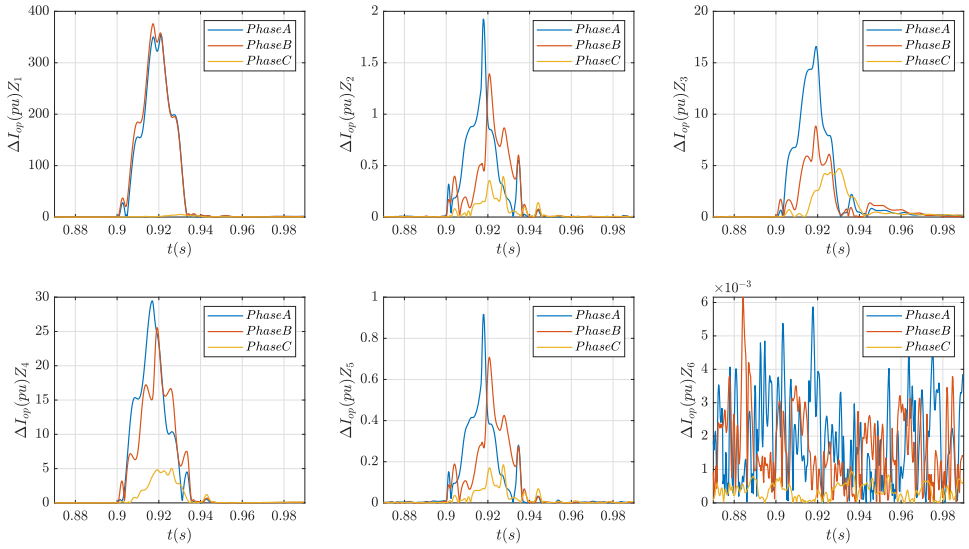

Figure 5.9. Short-circuit AB in Z1 in on-grid operation: $\Delta I_{op} \times t$

In addition, certain considerations emerge. Fig. 5.10 demonstrates satisfactory performance of the differential current, where it starts below the minimum threshold due to adaptive logic, swiftly entering the operational range, triggering a trip command at 0.90168 seconds, as shown in Figure 5.11.

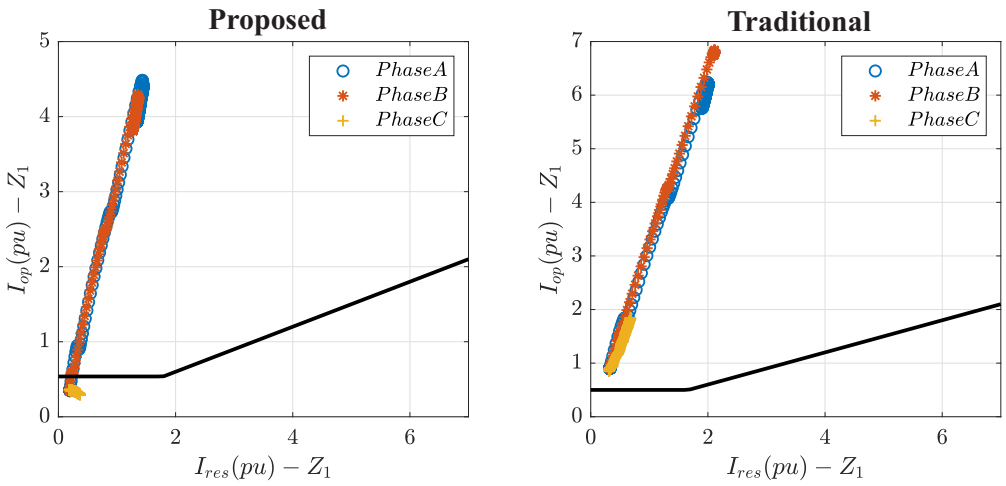

Figure 5.10. $I_{res}.SLP \times I_{op}$−Fault AB in Z1−$On - grid$.

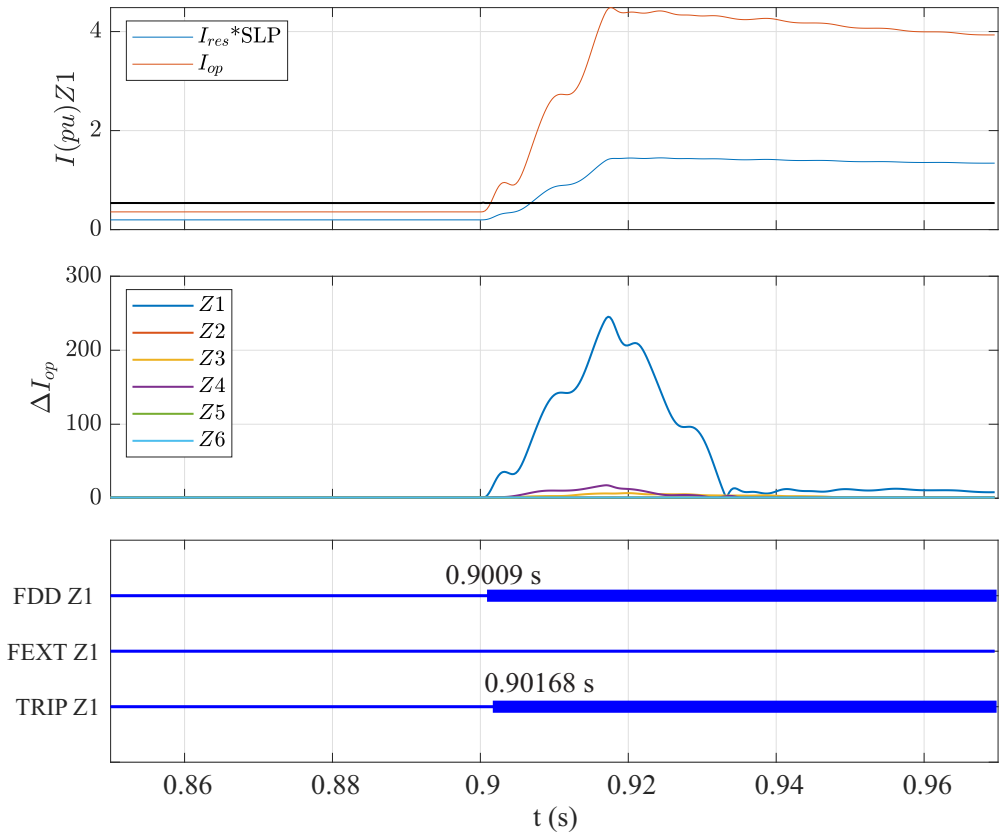

Figure 5.11. Case 01. Time domain response of the proposed function 87. On-grid operation.

Conversely, the traditional approach falters due to fixed threshold settings, lack of adaptive logic, and alterations in power flow caused by grid connection, resulting in relay misoperation. An external fault is identified at 0.93444 seconds following sensitization of the disturbance detector FDD, as depicted in Figure 5.12. It's worth noting that the performance of the proposed scheme remains uncompromised despite

the non-utilization of the CT on load L6.

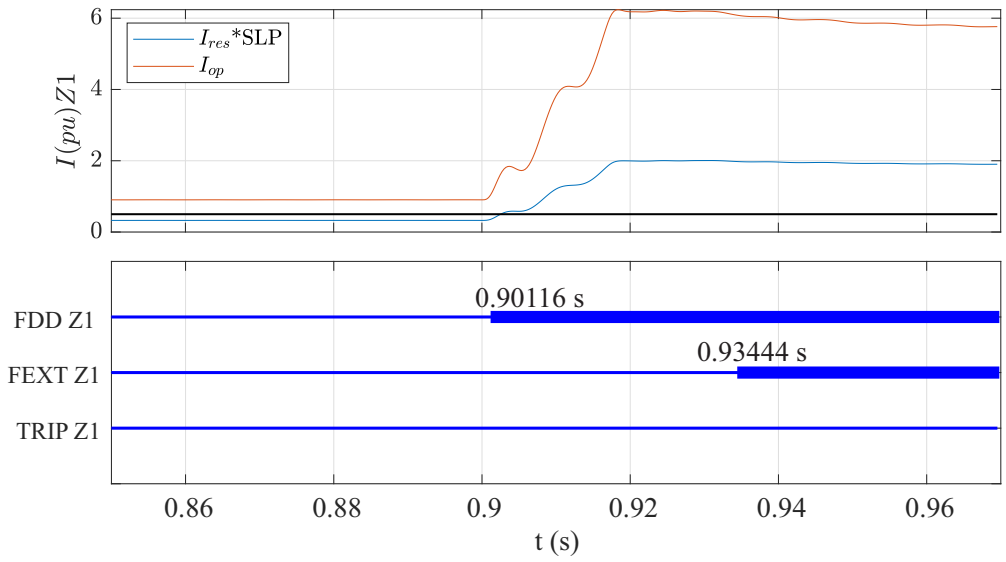

Figure 5.12. Case 01. Time domain response of the traditional function 87. On-grid operation.

5.4 CASE 2: SHORT-CIRCUIT AT DEAD ZONE

In this second case, the simulation was carried out in the dead zone, which is physically located in zone Z2, but logically lies between zones Z1 and Z2. Where it is located in a critical sector, which it is not covered by any main protection zone. Another fault occur also physically in Z2, and logically between Z2 and Z6. Both simulations works in order to validate the model and verify the advantages of using the differential relay in microgrids.

Thus, in this instance, a fault F2 in BC phases emerges at 0.9 seconds within the dead zone between CT2 and CB3. Another scenario involves a fault, F2b, occurring in the opposite dead zone between CB4 and CT6. These faults manifest during on-grid operation of the microgrid. Initially, examination of Figs. 5.13 and 5.14 reveals that the differential currents penetrate the operational region of protection zone Z2 similarly, i.e, the trip command to circuit breakers of the protection zone Z2 may be sent, because I_{op} enters in the operation zone. Thus, the logic states of the trip command and CBs of Z2 are 1 and 0, respectively.

The simulation triggers the opening of CBs within protection zone Z2 at the moment

indicated by vertical dashed lines in the figures 5.13 and 5.14. Notably, in the scenario where the fault arises close to CT2, which is shared with protection zone Z1, the CT2 currents in phases B and C surge following CB2 opening, besides CB3 from Z2 that already opened at the moment that the fault occurs.

Conversely, the corresponding currents of CT6 abruptly drop to zero. This response confirms the need to open protection zone Z1. In the second scenario, CT6 currents escalate post CBs opening, while CT2 currents diminish to zero, indicating the necessity to open CB11 in protection zone Z6.

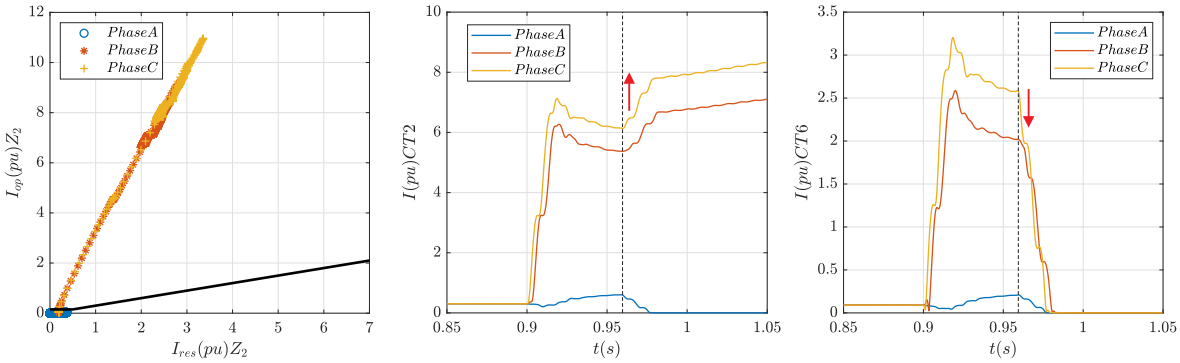

Figure 5.13. Case 2a: Fault if the dead zone close to CT2.

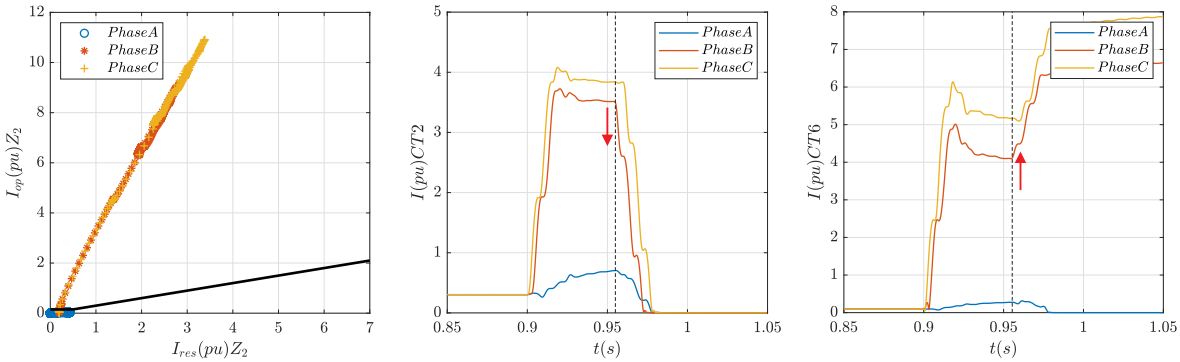

Figure 5.14. Case 2b: Fault if the dead zone close to CT6.

5.5 CASE 3: INFLUENCE OF FAULT RESISTANCE

In this scenario, or case 3, the microgrid is isolated from the main grid, leading to the occurrence of an AG fault in zone Z3 with fault resistances R_f set at 0 Ω , 25 Ω, and 50 Ω. To obtain stability, DG1 and DG2 operate in PQ mode, while DG3 and DG4 operate in V/f mode.

As illustrated in Fig. 5.15, the differential current initially falls below the minimum threshold but promptly enters the operation region following the fault. However, its amplitude decreases with higher fault resistances, as indicated in Fig. 5.15.a. This trend directly affects the time required to initiate the trip command, as illustrated in Fig. 5.15.b. Nonetheless, it's evident that the performance of the proposed method surpasses that of the traditional element.

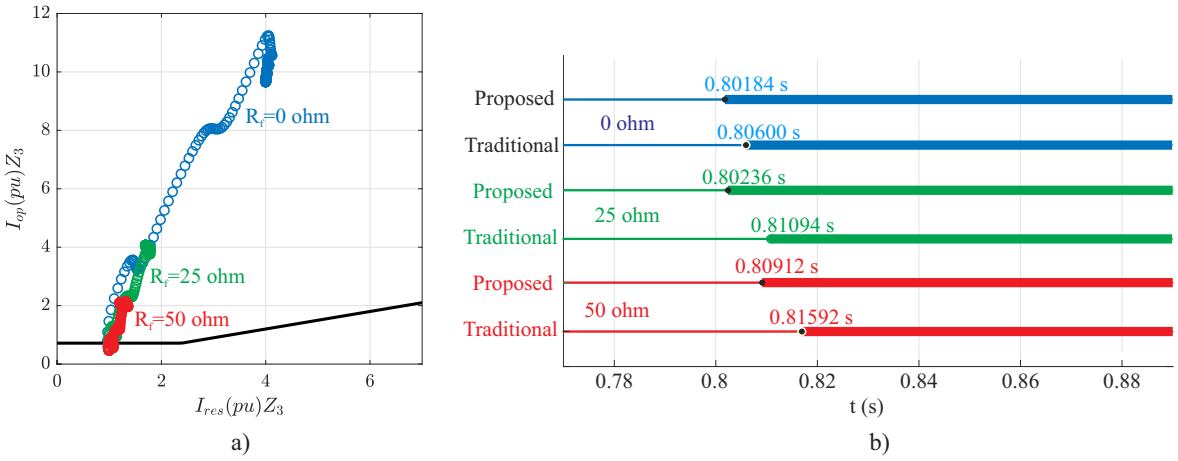

Figure 5.15. Case 3 - Fault resistance impact. (a) $I_res.SLP \times I_op$ $(b) Operation flags$.

Furthermore, Fig. 5.16 illustrates that the ratio between incremental operation currents within the faulted zone and other zones remains sufficiently high to ensure accurate identification of the faulted zone no matter what kind of fault resistance impedance occur, 0 Ω , 25 Ω, or 50 Ω.

This case demonstrates that the fault resistance can compromise the sensitivity of the conventional differential element, where the minimum threshold and slope determine the limit of relay sensitivity. However, by employing the strategy outlined in this study to adjust the minimum value based on power balance and incorporating the comparison of incremental currents, the algorithm's sensitivity can be enhanced.

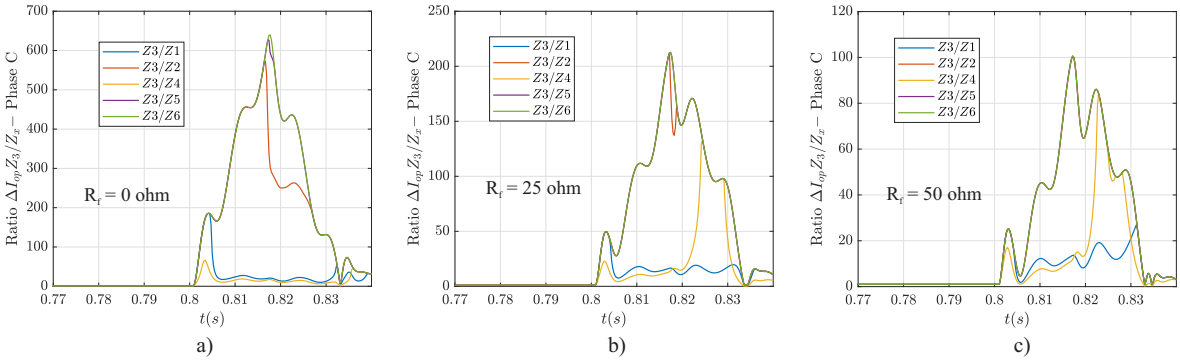

Figure 5.16. Case 3 - Fault resistance impact. (a) $I_res.SLP \times I_op$ $(b) Operation flags$.

5.6 CASE 4: FAULT TYPES

In this section, we simulated three fault types AG, ABG, and ABC within zone Z4 while the microgrid operated in off-grid mode. As predicted, the trajectory of ΔI_{op} entered the operation region in all three cases within Z4.

Conversely, it is observed that the other zones remained unaffected, except for zone Z3, by the closeness from Z4. Unlike single-phase faults, whose responses are depicted in Fig. 5.17, two-phase and three-phase faults can impact zone Z3 across the same faulted phases, as illustrated in Fig. 5.18 and 5.19, respectively.

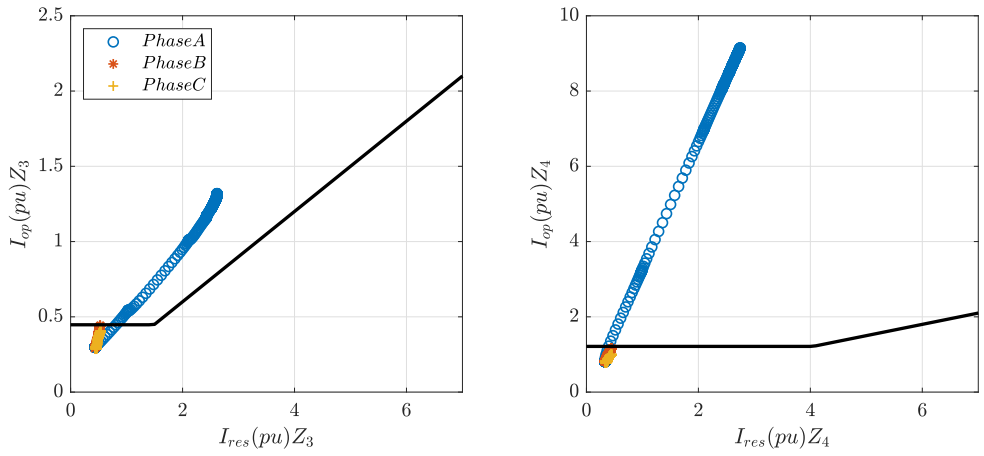

Figure 5.17. Case 04. Relay operation in zones Z3 and Z4 in case of a fault AG in Z4.

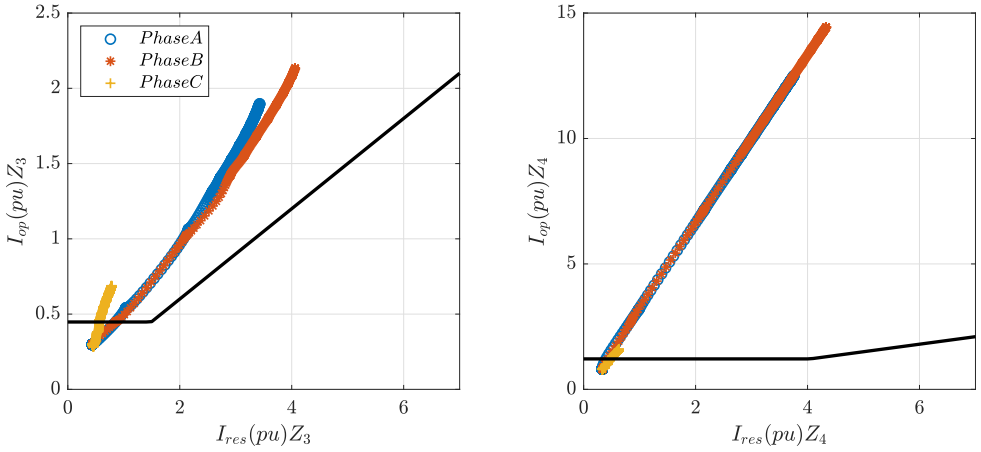

Figure 5.18. Case 04. Relay operation in zones Z3 and Z4 in case of an fault ABG in Z4.

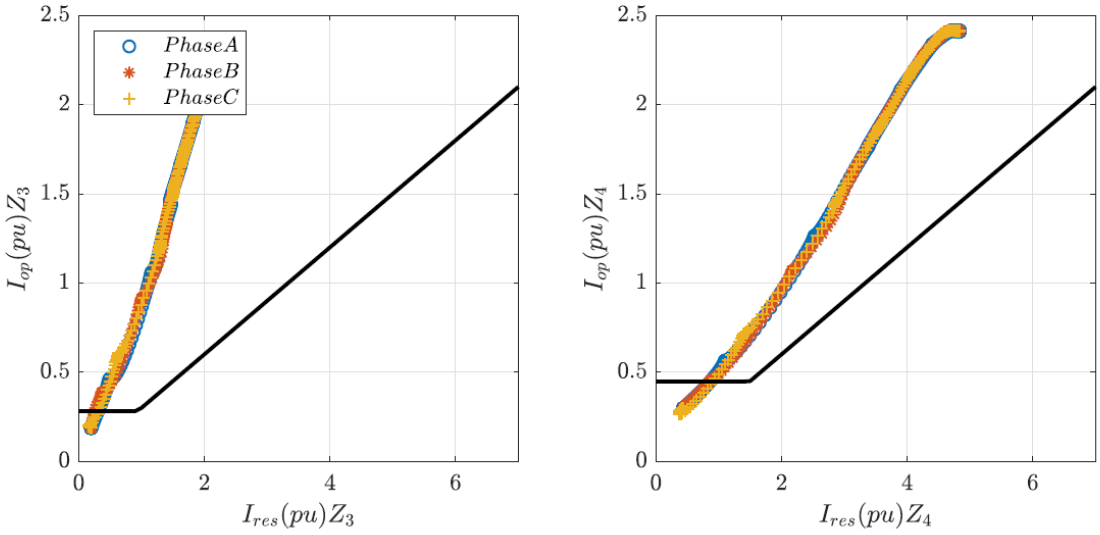

Figure 5.19. Case 04. Relay operation in zones Z3 and Z4 in case of fault ABC in Z4.

However, examining the ratio between ΔI_{op} of Z3 and Z4, as displayed in Figs. 5.20 and 5.21, assures the method's security. This is because $\Delta I_{op,Z4}$ for the faulted phases significantly exceeds $\Delta I_{op,Z3}3$ in both cases.

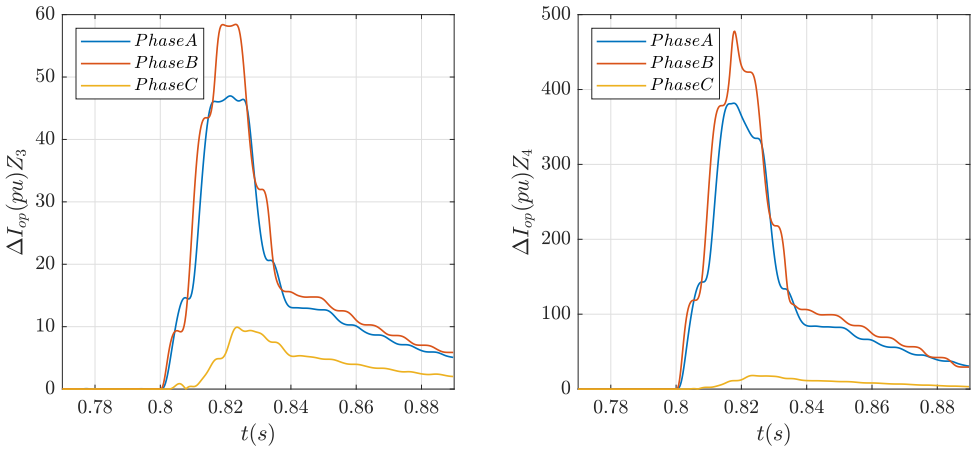

Figure 5.20. Case 04. Relay operation in zones Z3 and Z4 in case of a fault AG in Z4.

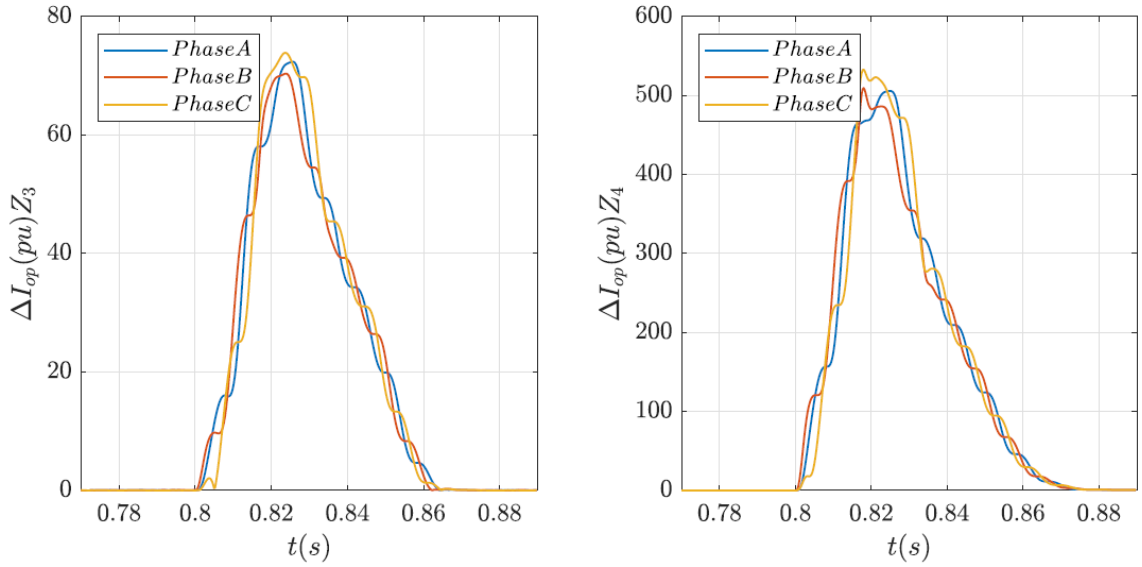

Figure 5.21. Case 04. Time-domain response of ΔI_op of Z3 and Z4 in case of a fault ABC in Z4.

5.7 CASE 5: RING AND RADIAL TOPOLOGY

In this next scenario, the simulated case changes the topology of the electrical grid. In order to obtain the effectiveness of the algorithm, a solid fault CG occurs at line DL5 during on-grid operation. For this case, the method is evaluated for both radial and ring topologies by altering the state of CB11 on Z6 (on and off).

Figs. 5.22 and 5.23 illustrate that the trajectories successfully enter the operation zone and are highly similar. To delve into this, it is crucial to observe in Fig. 5.23 that

initially, the module of the currents of CT4 and CT6 drops to zero upon the opening of CB6. Consequently, the currents of CT3 and CT1 increase while the CT5 current decreases, compared to the ring response illustrated in Fig. 5.22. Regardless of the topology used, the grid contribution remains consistent in both cases.

These responses suggest that the current entering CT4, equal to CT6, now flows through the transformers on the opposite side, CT1 and CT3. Consequently, the outgoing current, denoted as ΔI_{op}, remains approximately equal in both scenarios. Therefore, it is demonstrated that the reliability of the proposed technique remains unaffected by the topology of the microgrid.

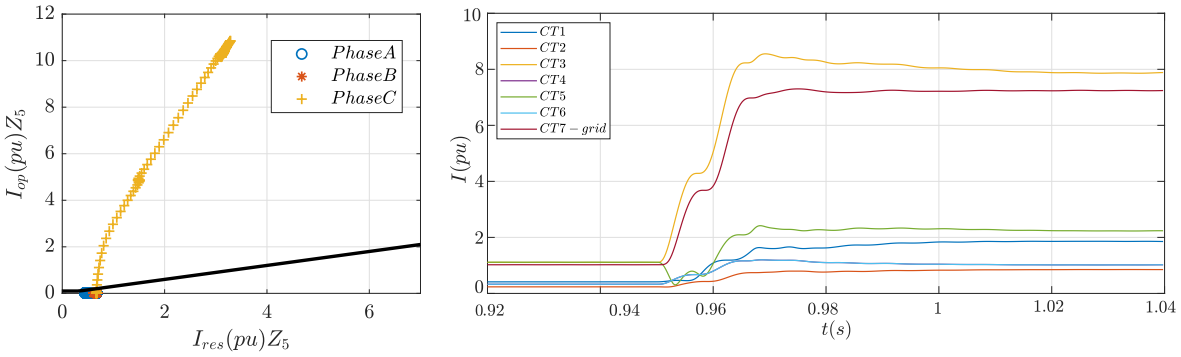

Figure 5.22. Case 05. Relay response for a CG fault in Z5 with a microgrid ring topology.

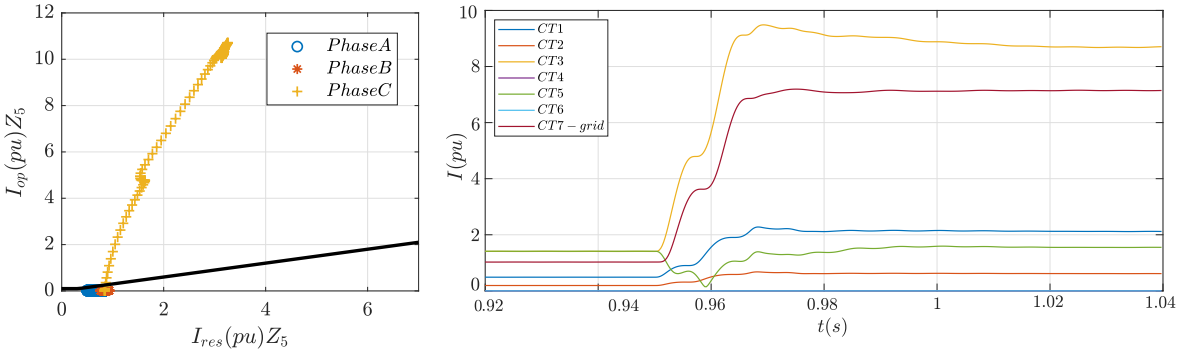

Figure 5.23. Case 05. Relay response for a CG fault in Z5 with a radial microgrid.

5.8 CASE 6: SIMULTANEOUS SHORT-CIRCUITS

In this scenario, simultaneous faults occur at different locations within the microgrid at different starting points. The microgrid operates in off-grid mode, with DG1 and DG2 functioning in PQ mode, while DG3 and DG4 operate in V/f mode. Initially, a

CT fault emerges at zone Z1 at 0.88 seconds, followed by a BC fault at 0.92 seconds in Z3. Fig. 5.24 illustrates that the CT fault in Z1 triggers the differential current to enter the operational region. Subsequently, when the BC fault occurs at Z3, both phase currents enter zone Z3, with the differential current of phase B sensitizing the differential current in Z1, even though it's not directly involved in the fault in this phase.

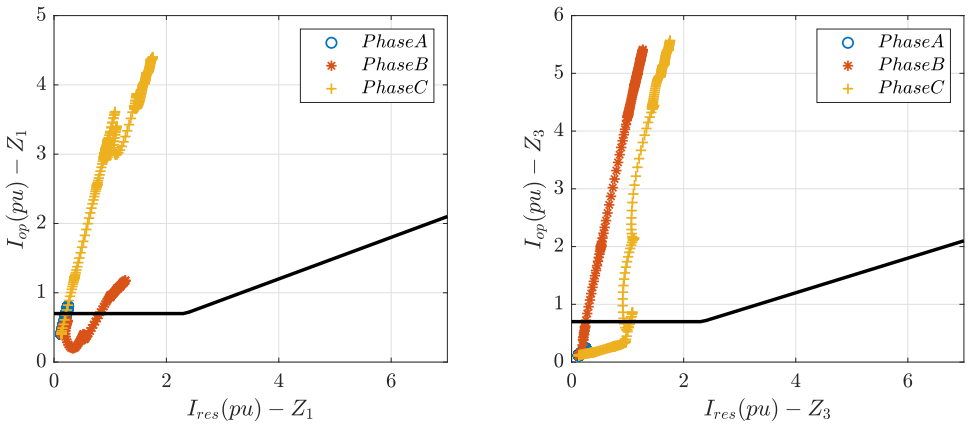

Figure 5.24. Case 06. Response in the traditional operational plane.

Fig. 5.25 confirms that the traditional element recognizes the initial fault at Z1. Additionally, it's noted that Z3 is sensitized due to the proximity between protection zones, classifying this disturbance as an external fault. Consequently, the relay fails to operate when the BC fault in Z3 occurs. However, Zone 1 in phase B is sensitized in response to the BC fault in Z3 without triggering an operation, as expected. Conversely, the relay correctly identifies the fault in Z3, as show in Fig. 5.26.

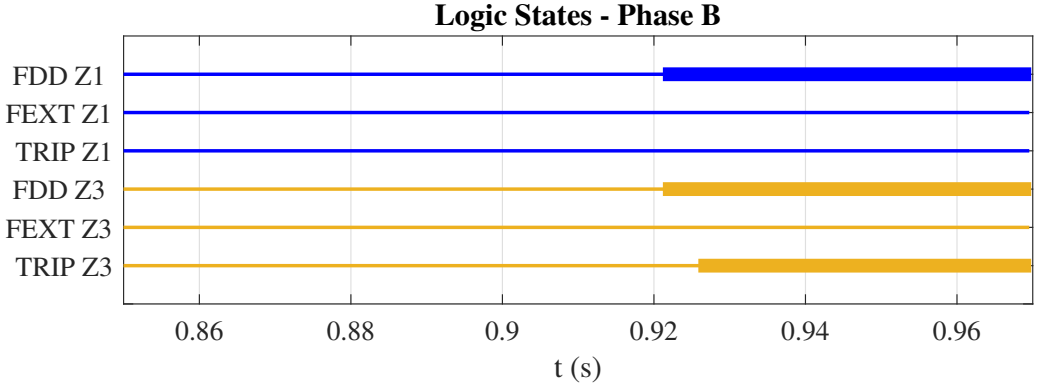

Figure 5.25. Case 06. Operation flags in phase B for the traditional 87 element.

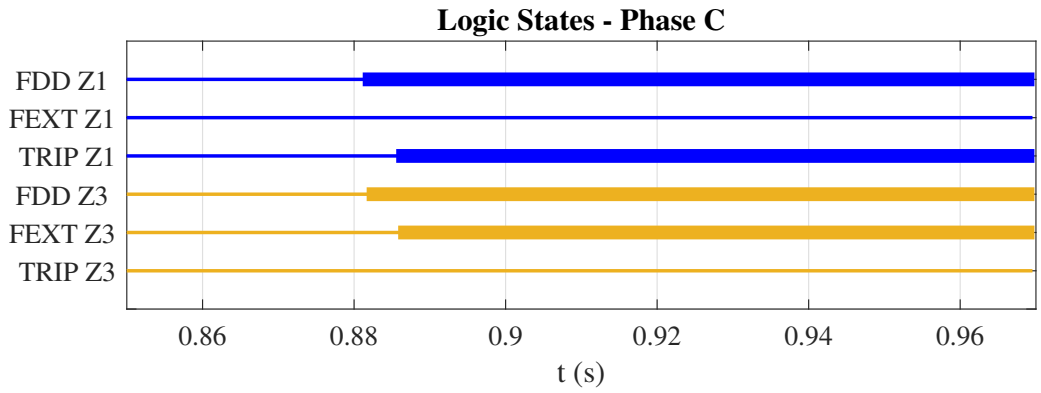

Figure 5.26. Case 06. Operation flags in phase C for the traditional 87 element.

Regarding the proposed technique, Fig. 5.27 demonstrates that, unlike the traditional element, the operating conditions in zone Z1 are not noticed for phase B, and the operation currents align coherently with the sequence of events. Conversely, Figs. 5.28 and 5.29 exhibit a successful response with reduced operation time. Specifically, the faults at Z3 are accurately recognized, as well as the fault of phase B in zone Z3.

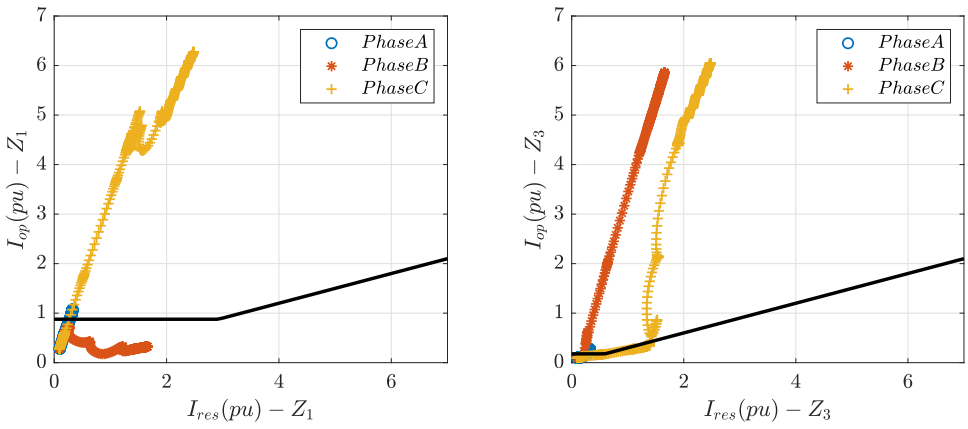

Figure 5.27. Case 06. Response in the operational plane of the proposed scheme.

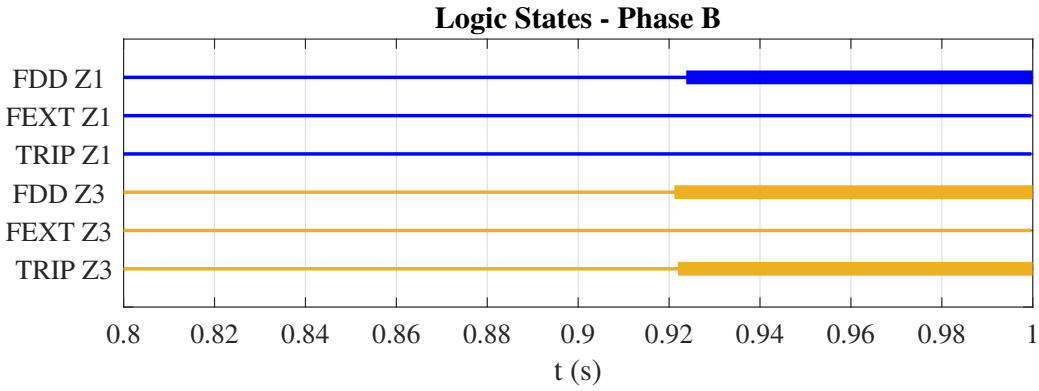

Figure 5.28. Case 06. Operation flags in phase B for the proposed 87 element.

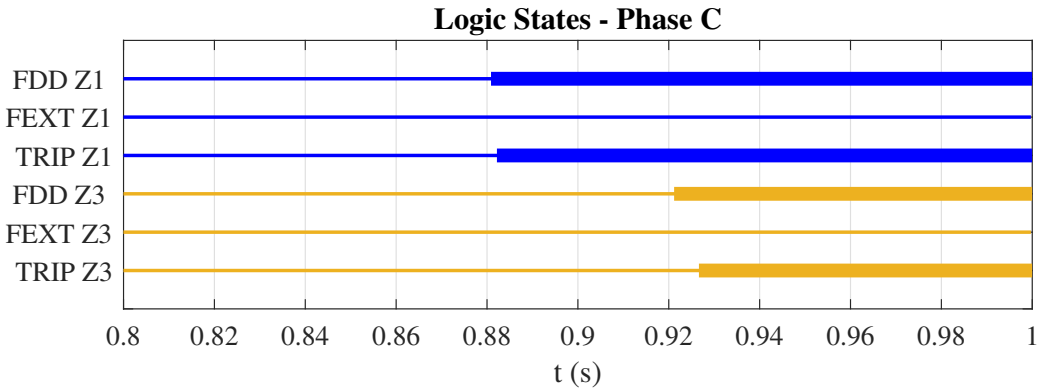

Figure 5.29. Case 06. Operation flags in phase C for the proposed 87 element.

Thus, two faults may occur at different locations with a time gap between their initiation moments. In such scenario, the conventional approach involves identifying the external fault by all unaffected protection zones and adjusting their settings accordingly. Setting the new slope value poses a challenge as it needs to be sensitive enough to detect internal faults during short-circuits elsewhere in the microgrid, yet uncertainty in microgrid operation makes this task difficult.

The proposed scheme addresses this issue by inherently recognizing the fault location through comparison of incremental differential currents. Furthermore, if two short-circuits occur in close proximity, the initial unaffected protection zone could be impacted. This implies that an external fault might be identified if the disturbance detector is overly sensitive but fails to meet operational conditions. Without backup protection logic, the relay could become blocked, compromising the security of the protection scheme.

5.9 CONTRIBUTIONS

Based on the results, some contributions of the proposed algorithm can be cited:

1. In conventional distribution networks, the number of CTs is higher because each distribution line has two terminal CTs, and each distributed generation also has its own CT, in addition to the use of CTs for load feeders. In the proposed differential protection, one CT per zone is used, and an additional CT per generation unit. This makes the proposed method much more affordable, without making the system less reliable and safe.

2. The minimum operating current is one of the main differential protection settings. This current avoids errors on the part of the CTs and measurement of the load leakage current, so current transformers are not necessary to supply the loads. Furthermore, CTs used with a differential element to measure the input contribution at the fault point and not the load current, which is why the minimum pickup can be constant, however, it is not suitable for microgrids as there is an intermittency between generation and charge.

3. The sensitivity of the relay to come into operation is related to the comparison between the incremental currents of the protection zones, which defines slope values. Thus, slope values that are too low can result in relay misoperation due to external faults, while high values can result in a delay in operation. The definition of the slope is essential to guarantee the sensitivity and the operating time of the differential current in the detection of internal faults.

4. In order to guarantee safety in the face of high CT saturation, a higher slope is traditionally placed, but in microgrids naturally, there is a lack of distributed generation outputs, which makes a scenario difficult to happen. However, simultaneous faults may occur in different locations. This aspect is not an actual concern for the proposed technique because the comparison between the incremental differential currents inherently recognizes where the fault does not occur. Moreover, if two faults are close, the initial non-faulted protection zone could

be affected. That means that an external fault would be identified if the disturbance detector was sensitized but without satisfying the operation conditions. If no backup protection logic was implemented, the relay may be blocked and the security of the protection scheme would be lost.

5. In a traditional differential element, the fault resistance can impair the sensitivity of disturbance detection. This sensitivity is defined by the slope and the minimum threshold. The strategy of changing the minimum value according to the power balance plus the comparison of differential incremental currents improves the sensitivity of the algorithm.

CHAPTER 6

CONCLUSIONS AND FUTURE WORKS

In this work, a protection function based on differential current is applied to active microgrids, complemented by an incremental element aiming to ensure reliability and security. To this purpose, a microgrid system modeled in EMTP software was used to carry out analyses of protection and operation behavior in the face of different situations such on-grid and off-grid operation and different topologies. The simulation of several short circuits with different characteristics at various locations in the microgrid allows to validate the effectiveness of the protection system. Then, the simplicity of its formulation, without the need for additional CTs compared to traditional systems, make it a suitable alternative for electric grids with distributed generation and loads.

Chapter 1 begins with a contextualization of the growth in the penetration of distributed generation in distribution networks, the benefits and disadvantages of this generation and a brief introduction of differential protection are presented. Chapter 1, also treats the objectives of the work and the publications carried out during the master's degree.

Chapter 2 presents a literature review of existing protection techniques for microgrid application. These techniques can be classified according with the basic concept, as current, frequency, voltage, impedance. After this review, it was verified that there is no a technique that works perfectly for all systems and for different situations, once the use of each method depends on the type of DG, the configuration of the network and the level of penetration.

Chapter 3 presents the theoretical background on the formulation of the differential protection of microgrid power systems. In addition, an overview of the operation modes of inverters according according with the status of the microgrid, i.e., on-grid or off-grid, is introduced. Also, typical control loops are presented.

Chapter 4 presents the formulation of the proposed relaying scheme is detailed. The main protection logic, the adaptive minimum pick-up logic, and the backup logic for dead zones are introduced. Thereafter, a brief description of the signal processing is done.

In Chapter 5, the analyses and results from the computer simulations were presented. Analyses for different situations that can be experienced, such as short-circuits at various points in the distribution network, in on-grid and off-grid operation, with fault resistances, using a ring or mesh topology and with the short-circuit occurring in the dead zone. Based on the results obtained, it can be concluded that the algorithm responds satisfactorily all situations, in relation to the speed, dependability and security.

Finally, one of the major contributions of this work was to demonstrate that the use of fewer current transformers, reducing the cost without losing the reliability and safety of the system, is possible, unlike conventional differential protection. Moreover, the differential element can dispense load feeders CTs. Additionally, the CTs utilized by the differential component are configured to accurately measure the incoming contribution at the fault location along the distribution line, with load currents being disregarded.

Based on this work and the results obtained, it is possible to propose improvements that can be addressed on future researches. Therefore, as a continuation of this work, it is suggested:

- Implement the proposed algorithm in a real device
- Test the protection algorithm for new alternative control schemes for inverters.
- Verify the algorithm performance considering the detailed model of converters, i.e., considering the switching transients.
- Use the developed model to test new protective function, like differential protection with voltage or frequency, wavelet transform.

BIBLIOGRAPHY

AGHDAM, T. S.; KAREGAR, H. K.; ZEINELDIN, H. H. Variable tripping time differential protection for microgrids considering dg stability. *IEEE Transactions on Smart Grid*, v. 10, n. 3, p. 2407–2415, 2019. Citado 4 vezes nas páginas 8, 11, 12, and 13.

ANUDEEP, B.; NAYAK, P. K. Differential power based selective phase tripping for fault-resilient microgrid. *Journal of Modern Power Systems and Clean Energy*, v. 10, n. 2, p. 459–470, 2022. Citado 4 vezes nas páginas 8, 11, 12, and 13.

CHEN, G.; LIU, Y.; YANG, Q. Impedance differential protection for active distribution network. *IEEE Transactions on Power Delivery*, v. 35, n. 1, p. 25–36, 2020. Citado 4 vezes nas páginas 9, 11, 12, and 13.

dos Reis, F. B.; PINTO, J. O. C.; dos Reis, F. S.; ISSICABA, D.; ROLIM, J. G. Multi-agent dual strategy based adaptive protection for microgrids. *Sustainable Energy, Grids and Networks*, v. 27, p. 100501, 2021. ISSN 2352-4677. Disponível em: <https://www.sciencedirect.com/science/article/pii/S2352467721000722>. Citado 4 vezes nas páginas 8, 11, 12, and 13.

DUA, G. S.; TYAGI, B.; KUMAR, V. Microgrid differential protection based on superimposed current angle employing synchrophasors. *IEEE Transactions on Industrial Informatics*, v. 19, n. 8, p. 8775–8783, 2023. Citado 4 vezes nas páginas 10, 11, 12, and 13.

DUBEY, K.; JENA, P. Impedance angle-based differential protection scheme for microgrid feeders. *IEEE Systems Journal*, v. 15, n. 3, p. 3291–3300, 2021. Citado 4 vezes nas páginas 6, 11, 12, and 13.

EL-SAYED, W. T.; EL-SAADANY, E. F.; ZEINELDIN, H. H. Interharmonic differential relay with a soft current limiter for the protection of inverter-based islanded microgrids. *IEEE Transactions on Power Delivery*, v. 36, n. 3, p. 1349–1359, 2021. Citado 4 vezes nas páginas 7, 11, 12, and 13.

FARINA, A. S. *CONTROLE DE MICRORREDE BASEADO EM FREQUÊNCIA*. 2018. Disponível em: <https://repositorio.utfpr.edu.br/jspui/bitstream/1/10099/1/CT_COELE_2018_1_02.pdf>. Citado na página 16.

HARON, A. R.; MOHAMED, A.; SHAREEF, H. Coordination of overcurrent, directional and differential relays for the protection of microgrid system. *Procedia Technology*, v. 11, p. 366–373, 2013. Disponível em: <https://api.semanticscholar.org/CorpusID:108814131>. Citado 4 vezes nas páginas 5, 11, 12, and 13.

HUANG, W.; NENGLING, T.; ZHENG, X.; FAN, C.; YANG, X.; KIRBY, B. J. An impedance protection scheme for feeders of active distribution networks. *IEEE*

Transactions on Power Delivery, v. 29, n. 4, p. 1591–1602, 2014. Citado 4 vezes nas páginas 6, 11, 12, and 13.

JIN, W.; ZHANG, S.; LI, J.; FENG, M.; FENG, S.; LU, Y. A novel differential protection scheme for distribution lines under weak synchronization conditions considering dg characteristics. *IEEE Access*, v. 11, p. 86561–86574, 2023. Citado 4 vezes nas páginas 7, 11, 12, and 13.

KHAN, M. A. U.; HONG, Q.; DYśKO, A.; BOOTH, C.; WANG, B.; DONG, X. Evaluation of fault characteristic in microgrids dominated by inverter-based distributed generators with different control strategies. p. 846–849, 2019. Citado na página 17.

LI, W.; TAN, Y.; LI, Y.; CAO, Y.; CHEN, C.; ZHANG, M. A new differential backup protection strategy for smart distribution networks: A fast and reliable approach. *IEEE Access*, v. 7, p. 38135–38145, 2019. Citado 3 vezes nas páginas 11, 12, and 13.

LIN XIAO MA, Z. W. Q. S. Z. L. Y. Y. Y. W. S. C. G. W. X. A novel current amplitude differential protection for active distribution network considering the source-effect of im-type unmeasurable load branches. *International Journal of Electrical Power Energy Systems*, v. 129, p. 0142–0615, 2021. Disponível em: <https://doi.org/10.1016/j.ijepes.2021.106780>. Citado 4 vezes nas páginas 6, 11, 12, and 13.

LIU, D.; DYśKO, A.; HONG, Q.; TZELEPIS, D.; BOOTH, C. D. Transient wavelet energy-based protection scheme for inverter-dominated microgrid. *IEEE Transactions on Smart Grid*, v. 13, n. 4, p. 2533–2546, 2022. Citado 4 vezes nas páginas 9, 11, 12, and 13.

LOUW, C.; BUQUE, C.; CHOWDHURY, S. Modelling and simulation of an adaptive differential current protection scheme for a solar pv microgrid. p. 1–7, 2014. Citado na página 2.

MANDITEREZA, P. T.; BANSAL, R. C. Protection of microgrids using voltage-based power differential and sensitivity analysis. *International Journal of Electrical Power Energy Systems*, v. 118, p. 105756, 2020. ISSN 0142-0615. Disponível em: <https://www.sciencedirect.com/science/article/pii/S014206151932900X>. Citado 4 vezes nas páginas 9, 11, 12, and 13.

MIAO, X.; ZHAO, D.; LIN, B.; JIANG, H.; CHEN, J. A differential protection scheme based on improved dtw algorithm for distribution networks with highly-penetrated distributed generation. *IEEE Access*, v. 11, p. 40399–40411, 2023. Citado 4 vezes nas páginas 8, 11, 12, and 13.

NIKOLAIDIS, V. C.; MICHALOUDIS, G.; TSIMTSIOS, A. M.; TZELEPIS, D.; BOOTH, C. D. A coordinated multi-element current differential protection scheme for active distribution systems. *IEEE Transactions on Power Delivery*, v. 37, n. 5, p. 4261–4271, 2022. Citado 4 vezes nas páginas 9, 11, 12, and 13.

NSENGIYAREMYE, J.; PAL, B. C.; BEGOVIC, M. M. Microgrid protection using low-cost communication systems. *IEEE Transactions on Power Delivery*, v. 35, n. 4, p. 2011–2020, 2020. Citado 4 vezes nas páginas 8, 11, 12, and 13.

ONS. Plano diretor de Desenvolvimento tecnológico. Rio de Janeiro, Brasil. [S.l.], 2020. Citado na página 1.

ONS. Relatório Anual de Sustentabilidade 2022. Rio de Janeiro, Brasil. [S.l.], 2022. Citado na página 1.

ROCABERT, J.; LUNA, A.; BLAABJERG, F.; RODRíGUEZ, P. Control of power converters in ac microgrids. *IEEE Transactions on Power Electronics*, v. 27, n. 11, p. 4734–4749, 2012. Citado na página 17.

RODRIGUES, I. R. A. *Estudo de proteção elétrica de uma microrrede baseada na rede de 34 barras do IEEE*. 2017. Disponível em: <http://hdl.handle.net/1843/BUOS-AVAFMX>. Citado na página 16.

SAMAL, S.; SAMANTARAY, S. R.; SHARMA, N. K. Data-mining model-based enhanced differential relaying scheme for microgrids. *IEEE Systems Journal*, v. 17, n. 3, p. 3623–3634, 2023. Citado 4 vezes nas páginas 10, 11, 12, and 13.

SOLEIMANISARDOO, A.; KAREGAR, H. K.; ZEINELDIN, H. H. Differential frequency protection scheme based on off-nominal frequency injections for inverter-based islanded microgrids. *IEEE Transactions on Smart Grid*, v. 10, n. 2, p. 2107–2114, 2019. Citado 4 vezes nas páginas 6, 11, 12, and 13.

USTUN, T. S.; KHAN, R. H. Multiterminal hybrid protection of microgrids over wireless communications network. *IEEE Transactions on Smart Grid*, v. 6, p. 2493–2500, 2015. Disponível em: <https://api.semanticscholar.org/CorpusID:21887176>. Citado 4 vezes nas páginas 6, 11, 12, and 13.

USTUN, T. S.; OZANSOY, C.; ZAYEGH, A. Differential protection of microgrids with central protection unit support. p. 15–19, 2013. Citado 2 vezes nas páginas 14 and 15.

WHEELER, K. A.; FARIED, S. O.; ELSAMAHY, M. A microgrid protection scheme using differential and adaptive overcurrent relays. p. 1–6, 2017. Citado na página 1.

ZHOU, C.; ZOU, G.; DU, X.; ZANG, L. Adaptive current differential protection for active distribution network considering time synchronization error. *International Journal of Electrical Power Energy Systems*, v. 140, p. 108085, 2022. ISSN 0142-0615. Disponível em: <https://www.sciencedirect.com/science/article/pii/S0142061522001272>. Citado 4 vezes nas páginas 6, 11, 12, and 13.

ZHOU, C.; ZOU, G.; ZANG, L.; DU, X. Current differential protection for active distribution networks based on improved fault data self-synchronization method. *IEEE Transactions on Smart Grid*, v. 13, n. 1, p. 166–178, 2022. Citado 4 vezes nas páginas 7, 11, 12, and 13.

ZHOU, C.; ZOU, G.; ZHANG, S.; ZHENG, M.; TIAN, J.; DU, T. Mathematical morphology-based fault data self-synchronization method for differential protection in distribution networks. *IEEE Transactions on Smart Grid*, v. 14, n. 4, p. 2607–2620, 2023. Citado 4 vezes nas páginas 7, 11, 12, and 13.